



Variability in oxygen isotopic fractionation of enzymatic O₂ consumption

Carolina F. M. de Carvalho¹, Moritz F. Lehmann¹, Sarah G. Pati^{1,2}

¹ Department of Environmental Sciences, University of Basel, 4056 Basel, Switzerland

5 ² Department of Environmental Geosciences, Centre for Microbiology and Environmental Systems Science, University of Vienna, 1090 Vienna, Austria

Correspondence to: Sarah G. Pati (sarah.pati@univie.ac.at)

Abstract. Stable isotope analysis of O₂ has emerged as a valuable tool to study O₂ dynamics at various environmental scales, from molecular mechanisms to ecosystem processes. Despite its utility, there is a lack of fundamental understanding of the large variability observed in O₂ isotopic fractionation at the environment- and even enzyme-level. To expand our knowledge on the potential causes of this variability, we determined ¹⁸O-kinetic isotope effects (KIEs) across a broad range of O₂-consuming enzymes. The studied enzymes included nine flavin-dependent, five copper-dependent, and one copper-heme-dependent oxidases, as well as one flavin-dependent monooxygenase. For twelve of these enzymes, ¹⁸O-KIEs were determined for the first time. The comparison of ¹⁸O-KIEs, determined in this and previous studies, to calculated ¹⁸O-equilibrium isotope effects revealed distinct patterns of O-isotopic fractionation within and between enzyme groups, reflecting differences in active-site structures and O₂-reduction mechanisms. Flavin-dependent O₂-consuming enzymes exhibited two distinct ranges of ¹⁸O-KIEs (from 1.020 to 1.034 and from 1.046 to 1.058), likely associated with the rate-limiting steps of two different O₂-reduction mechanisms (sequential vs. concomitant 2-electron transfer). In comparison, iron- and copper-dependent enzymes displayed a narrower range of ¹⁸O-KIEs, with overall lower values (from 1.009 to 1.028), which increased with the degree of O₂ reduction during the rate-limiting step. Similar to flavin-dependent O₂-consuming enzymes, copper-dependent O₂-consuming enzymes also featured two main, yet narrower, ranges of ¹⁸O-KIEs (from 1.009 to 1.010 and from 1.017 to 1.022), likely associated with the rate-limiting formation of a copper-superoxo or copper-hydroperoxo intermediate. Overall, our findings support generalizations regarding expected ¹⁸O-KIEs ranges imparted by O₂-consuming enzymes and have the potential to help interpret stable O₂ isotopic fractionation patterns across different environmental scales.

25 1 Introduction

Stable isotope analysis of O₂ has proven to be a valuable tool for tracking and quantifying environmentally relevant O₂ dynamics across different spatial and temporal scales. On a large environmental scale, stable isotope analysis of O₂ has been most commonly used in aquatic studies to estimate the productivity of oceans and lakes (Luz and Barkan 2000; Hendricks et al. 2005; Gammons et al. 2014; Bocaniov et al. 2015; Bogard et al. 2017), but also as a tracer of ocean circulation (Kroopnick and Craig 1976; Bender 1990; Levine et al. 2009), and to estimate historical changes in the global hydrological and O₂ cycle



(Petit et al. 1999; Severinghaus et al. 2009; Blunier et al. 2012). On a smaller environmental scale, it has been used to study the dynamics of O₂ consumption by plants (Guy et al. 1992, 1993; Ribas-Carbo et al. 1995; Helman et al. 2005), microorganisms (Helman et al. 2005; Stolper et al. 2018; Ash et al. 2020), and humans (Epstein and Zeiri 1988; Zanonato et al. 1992).

35 In most environmental applications of O₂ isotope analysis, biological O₂ consumption is the main process driving and modulating the changes in the ¹⁸O/¹⁶O and ¹⁷O/¹⁶O ratios of O₂. Spatial and/or temporal changes in O₂ isotope ratios are referred to as isotopic fractionation and can be quantified with, for example, ¹⁸ε values (see Eq. (1)) (Coplen 2011):

$$^{18}\epsilon = \ln\left(\frac{(^{18}\text{O}/^{16}\text{O})}{(^{18}\text{O}/^{16}\text{O})_0}\right) / \ln\left(\frac{[\text{O}_2]}{[\text{O}_2]_0}\right) \quad (1)$$

Here, (¹⁸O/¹⁶O) and (¹⁸O/¹⁶O)₀ represent the isotopic ratios of O₂ in a sample at a given timepoint, and in a reference sample
40 (typically reflecting initial conditions or original source), respectively, and [O₂]/[O₂]₀ represents the fraction of O₂ remaining after partial consumption. Typically, ¹⁸ε values are indicative of a specific reactive process and may thus be used to identify, track, and quantify O₂ consumption processes in the environment. However, the magnitude of ¹⁸ε values measured for bulk biological O₂ consumption, considered to be predominantly respiration, varies considerably. Specifically, in aquatic environments, ¹⁸ε values determined for respiratory O₂ consumption range from -7 ‰ to -26 ‰ (Kiddon et al. 1993; Helman
45 et al. 2005; Wang et al. 2008; Levine et al. 2009; Bocaniov et al. 2015). Although it has been suggested that the observed variability in ¹⁸ε values can be explained by the different types of organisms consuming O₂, the availability of light (e.g. effect of photosynthesis and/or photoinhibition pathways) and the main metabolic pathway (Mader et al. 2017), there is still no fundamental understanding of the underlying causes of this variability. The uncertainty associated with the O-isotopic fractionation of respiratory O₂ consumption has substantial implications for the application of O₂ isotope analysis to study
50 ecosystem respiration on an environmental scale. For instance, most O₂-isotope applications to study aquatic ecosystems require assuming a constant ¹⁸ε value for respiration to estimate respiration rates (Wang et al. 2008; Bocaniov et al. 2012; Bogard et al. 2017). Consequently, these respiration rates are prone to considerable error depending on the accuracy of chosen community respiration ¹⁸ε value (Hotchkiss and Hall 2014).

To improve the quantification of gross O₂ production in aquatic environments, an increasing number of studies are
55 applying the triple oxygen isotope (TOI) method (Luz and Barkan 2000; Hendricks et al. 2005; Juranek and Quay 2013; Jurikova et al. 2016). In TOI applications, changes in ¹⁷O/¹⁶O ratios relative to changes in ¹⁸O/¹⁶O ratios along O₂ concentration gradients are quantified as λ values (Miller 2002; Sharp et al. 2018). λ values for biological O₂ consumption range between 0.51 and 0.53 (Young et al. 2002; Luz and Barkan 2005; Ash et al. 2020; Hayles and Killingsworth 2022), with a value of 0.518 typically assumed for marine respiration (Luz and Barkan 2009; Juranek and Quay 2013). Because λ values vary less
60 than ¹⁸ε values for respiration, TOI analysis often improves gross O₂ production estimates. However, the overall robustness of λ values representative for respiration, and other biological O₂-consuming processes, has been recently questioned in other studies (Stolper et al. 2018; Ash et al. 2020; Sutherland et al. 2022a, 2022b).



In addition to environmental applications, stable isotope analysis of O₂ has also been applied on a molecular scale to uncover reaction mechanisms of substrate oxidation and O₂ reduction by O₂-consuming enzymes (Roth and Klinman 2005). Specifically, oxygen equilibrium isotope effects (¹⁸O-EIEs) and oxygen kinetic isotope effects (¹⁸O-KIEs) are used as mechanistic probes to assess the rate-limiting steps in O₂-consuming enzymatic reactions (Roth and Klinman 2005). ¹⁸O-EIEs can be calculated or experimentally determined for the reversible formation of free, or ligand-bound, reactive oxygen species (Roth and Klinman 2005; Lanci et al. 2007; Mirica et al. 2008), such as superoxide (O₂^{•-}, see Eq. (2)), and reflect the ratio of reaction rate constants of light (¹⁶O¹⁶O) versus heavy (¹⁸O¹⁶O) isotopologues of O₂, as shown in Eq. (3).



$$^{18}\text{O-EIE} = \frac{^{18}\text{O-KIE}_f}{^{18}\text{O-KIE}_r} = \frac{^{16}k_f/^{18}k_f}{^{16}k_r/^{18}k_r} \quad (3)$$

Where k_f and $^{18}\text{O-KIE}_f$ are the reaction rate constant and KIE of the forward reaction between O₂ and O₂^{•-}, k_r and $^{18}\text{O-KIE}_r$ are the reaction rate constant and KIE of the reverse reaction, and ^{16}k and ^{18}k denote reaction rate constants for the light and heavy isotopologues of O₂, respectively. Experimentally determined ¹⁸O-KIEs reflect the O-isotopic fractionation occurring in all elementary reaction steps up to, and including, the rate-limiting step (Roth and Klinman 2005). Experimental ¹⁸O-KIEs are thus often referred to as observable or apparent ¹⁸O-KIEs, and they reflect an averaged O-isotope effect for both O atoms in O₂. Apparent ¹⁸O-KIEs are related to ¹⁸ε values as shown in Eq. (4).

$$^{18}\text{O-KIE} = (^{18}\epsilon + 1)^{-1} \quad (4)$$

Typically, apparent ¹⁸O-KIEs closely reflect the intrinsic ¹⁸O-KIE of the rate-limiting step, which can be the binding of O₂ to the active site, or an elementary O₂ reduction step (Roth and Klinman 2005). Because intrinsic ¹⁸O-KIEs cannot be easily calculated, ¹⁸O-EIEs are often used as a reference to assign experimentally determined ¹⁸O-KIEs to a specific rate-limiting step (Roth and Klinman 2005). Together, these parameters can help to elucidate the intermediate species, and the number of electrons and protons transferred to O₂, before and during the rate-limiting step (Roth and Klinman 2003; Mirica et al. 2008; Humphreys et al. 2009).

All biological O₂ consumption, including respiration, detoxification, and biosynthesis, is ultimately carried out by O₂-consuming enzymes. Therefore, the variability in the isotopic fractionation of O₂ observed at both small and large environmental scales may be initially attributed to that observed at the enzyme level. However, few attempts have been made to relate O₂ isotopic fractionation occurring at the enzyme level to that occurring at larger environmental scales (Guy et al. 1987, 1989). So far, approximately 850 O₂-consuming enzymes have been described by *The Nomenclature Committee of the International Union of Biochemistry and Molecular Biology database* (McDonald et al. 2009). Yet, comparatively few have



been comprehensively studied. O₂-consuming enzymes have evolved specialized active-site structures to overcome the kinetic limitations of O₂ reduction and to exploit the reactivity of the reduced oxygen species for productive redox catalysis (Malmstrom 1982; Klinman 2007; Frey and Hegeman 2007). These active site structures are typically flavin-, copper- or iron-dependent structures that, via the formation of radical intermediates with organic cofactors, or interactions with transition-state metals, can rapidly and easily reduce O₂ (Malmstrom 1982; Bugg 2001; Bento et al. 2006; Frey and Hegeman 2007; Pimviriyakul and Chaiyen 2020). There are two major groups of O₂-consuming enzymes: oxidases and oxygenases. Oxidases catalyze the transfer of one-, two-, or four-electrons from their substrate(s) to O₂, reducing O₂ to either hydrogen peroxide (H₂O₂) or water (H₂O) (Malmstrom, 1982). The transfer of electrons from a given substrate to O₂ typically occurs in two separate steps through oxidation and reduction of the enzyme. Substrate oxidation by the oxidized enzyme occurs in the reductive half-reaction, and O₂ reduction by the reduced enzyme occurs in the oxidative half-reaction. Oxidases are more often involved in catabolic processes, oxidizing substrates like alcohols, amines, and amino acids (Medda et al. 1995; Finney et al. 2014; Pimviriyakul and Chaiyen 2020). For example, glucose oxidase, one of the most well studied oxidases, catalyzes the oxidation of β-D-glucose to D-glucono-δ-lactone and H₂O₂. This reaction is part of the catabolic process that breaks down glucose, providing energy and components needed for anabolic reactions (Bauer et al. 2022). Oxygenases, on the other hand, catalyze the incorporation of one, or both, oxygen atoms of O₂ into their substrate(s), and are consequently referred to as mono- or dioxygenases, respectively. As such, O₂ reduction typically co-occurs with substrate oxidation and often requires external electron donors, such as NAD(P)H. Oxygenases can catalyze a broader range of substrates, including aromatic hydrocarbons and fatty acids, and are primarily involved in biosynthesis and detoxification (Bugg 2001; Bernhardt 2006; van Berkel et al. 2006). For example, cytochrome P450 enzymes represent a superfamily of monooxygenases found in all domains of life, which play a vital role in the biosynthesis of steroids, fatty acids, and bile acids, as well as the inactivation of drugs, toxins, and environmental pollutants (Guengerich 2007). To the best of our knowledge, enzymatic ¹⁸O-KIEs have been experimentally determined for only 26 O₂-consuming enzymes, with values ranging from 1.009 to 1.053 (Guy et al. 1989; Cheah et al. 2014, see full list of references in Table S1 of the supplement). This range in enzymatic ¹⁸O-KIEs is equivalent to a range in ¹⁸ε values of -9 ‰ to -50 ‰, significantly exceeding the previously mentioned range of ¹⁸O-ε values observed for respiratory O₂ consumption (Mader et al. 2017). Most of these enzymatic ¹⁸O-KIEs have been determined with the primary goal to understand specific enzymatic reaction mechanisms of O₂ reduction and substrate oxidation. Comprehensive investigations into the O-isotopic fractionation of enzymatic O₂ consumption, which specifically aim at understanding the underlying causes of the observed variability in ¹⁸O-KIEs, are lacking.

To expand and improve our understanding of the variability in isotopic fractionation of O₂ at the enzyme level, this study reports 19 experimentally determined ¹⁸O-KIEs for nine flavin-dependent, five copper-dependent, and one copper-heme-dependent oxidase, as well as for one flavin-dependent monooxygenase. In a first step, enzyme assays were conducted to determine initial O₂ consumption rates and Michaelis-Menten kinetic constants of each enzymatic reaction to establish saturating substrate concentrations and the presence or absence of product or substrate inhibition. Subsequently, experiments to determine characteristic ¹⁸O-KIEs were carried out under optimized conditions for each enzyme, whenever possible. For



125 selected enzymes, additional ^{18}O -KIEs were measured using alternative substrates, or under limiting O_2 concentrations, to
assess the influence of these variables on the variability of single-enzyme ^{18}O -KIEs. The combined analysis of ^{18}O -KIEs of
 O_2 -consuming enzymes determined in this and previous studies allowed a comprehensive assessment of the variability of
isotope effects both within the same active-site structure and across different active-site structures. Our findings not only
improve the interpretation and generalization of isotopic fractionation of O_2 at the enzyme level, but also contribute to a deeper
130 understanding of the origins of variations in O_2 isotopic fractionation at the organism and environmental levels. Ultimately,
this research supports the application of stable O_2 -isotope analysis as a useful and robust tool for investigating O_2 -
biogeochemical dynamics from molecular to ecosystem scales.

2 Materials and Methods

2.1 Chemicals and enzymes

135 Unless noted otherwise, enzymes (see list in Table 1) and chemicals were purchased from Sigma-Aldrich and used as received.
Sodium phosphate dibasic (Na_2HPO_4 , 99%, Carl Roth), sodium phosphate monobasic dihydrate ($\text{NaH}_2\text{PO}_4 \cdot 2\text{H}_2\text{O}$, 99%,
Merck), sodium acetate (98.5%, Carl Roth), 2-amino-2-(hydroxymethyl)-1,3-propanediol (Tris, 99%), *N*-2-
hydroxyethylpiperazine-*N'*-2-ethane-1-sulphonic acid sodium salt (HEPES, 99%, Carl Roth), sodium hydroxide (NaOH , 98%),
and hydrochloric acid (HCl , 37%, VWR) were used to make buffer solutions. Sodium chloride (NaCl , 99.5%, Carl Roth),
140 potassium chloride (KCl , 99%), thiamine diphosphate (95%), manganese sulfate (MnSO_4 , 99%, Carl Roth), flavin adenine
dinucleotide disodium salt hydrate (FAD, 95%), DL-dithiothreitol (99%), Thesit® (non-ionic surfactant for membrane
research), and isopropanol (HPLC grade, Carl Roth) were added to certain enzyme assays to increase enzymatic activity or
substrate solubility. Methanol (99.9%, Carl Roth), ethanol (99.8%, Honeywell), L-ascorbic acid (98%), bilirubin (98%),
cholesterol (99%), choline chloride (98%), cytochrome-*c* from bovine heart (95%), D-alanine (98%), histamine
145 dihydrochloride (99%), D-(+)-glucose (99.5%), D-(+)-mannose (99%), L-kynurenine (98%), β -nicotinamide adenine
dinucleotide phosphate reduced tetrasodium salt hydrate (NADPH, 95%), hydroquinone (99%), 2,2'-Azino-bis(3-
ethylbenzothiazoline-6-sulfonic acid) diammonium salt (ABTS, 98%), L-(+)-lactic acid (98%), L-lysine monohydrochloride
(99.5%), sodium pyruvate (99%), and sarcosine (98%) were used as (co)substrates. Hydrogen peroxide (H_2O_2 , 30%),
formaldehyde (36%), acetaldehyde (99.5%), betaine (98%), ammonium chloride ($\geq 99\%$), *p*-benzoquinone (98%), sodium
150 bicarbonate (99.5 %), and glycine (98.5%) were used to test product inhibition of enzymatic activities. Sodium sulfite (Na_2SO_3 ,
98%) was used to calibrate optical oxygen sensors. All solutions were made in ultrapure water (18.2 $\text{M}\Omega$ cm, ELGA
LabWater). O_2 (99.995%), N_2 (99.999%), and He (99.999%) gas were from Carbagas AG.



155 **Table 1. Names, Enzyme Commission (EC) numbers, biological sources, and activities of all enzymes used in this study.**

Enzyme name	EC no.	Source	Activity ^a
alcohol oxidase	1.1.3.13	<i>Pichia pastoris</i>	24
L-ascorbate oxidase	1.10.3.3	<i>Cucurbita sp.</i>	1257
bilirubin oxidase	1.3.3.5	<i>Myrothecium verrucaria</i>	33
cholesterol oxidase	1.1.3.6	microorganisms	99
choline oxidase	1.1.3.17	<i>Arthrobacter sp.</i>	16-19 ^b
cytochrome-c oxidase	7.1.1.9	bovine heart	33
D-amino-acid oxidase	1.4.3.3	porcine kidney	12
diamine oxidase	1.4.3.22	porcine kidney	0.0008-0.0018 ^{b,c}
glucose oxidase	1.1.3.4	<i>Aspergillus niger</i>	305
kynurenine 3-monooxygenase	1.14.13.9	<i>Pseudomonas fluorescens</i>	7000000 ^c
laccase	1.10.3.2	<i>Agaricus bisporus</i>	32 ^c
laccase	1.10.3.2	<i>Trametes versicolor</i>	0.9 ^c
L-lactate oxidase	1.1.3.2	<i>Aerococcus viridians</i>	40 ^c
L-lysine oxidase	1.4.3.14	<i>Trichoderma viride</i>	39
pyruvate oxidase	1.2.3.3	<i>Aerococcus sp.</i>	89
sarcosine oxidase	1.5.3.1	<i>Bacillus sp.</i>	50 ^c

^a in $\mu\text{mol min}^{-1} (\text{mg protein})^{-1}$ (unless indicated otherwise) determined under specific conditions defined by the manufacturer

^b multiple batches of enzyme with different activities were used

^c activity is reported per mg total solid instead of per mg protein

160 2.2 Enzyme assays for kinetic parameters

To measure (initial) O_2 consumption rates, enzyme assays were performed in clear glass, crimp-top vials with a volume of 9 mL when closed. These vials contained small magnetic stir bars, were filled headspace-free with assay solution, and closed with hollow butyl rubber stoppers and crimp caps. Assay solutions consisted of an air-equilibrated buffer, an organic substrate, cofactors and co-substrates if necessary, and the respective enzyme of interest (see Appendix A for details). Once filled and closed, vials were placed on a magnetic stirring plate at room temperature ($23 \pm 1^\circ\text{C}$). Enzymatic reactions were initiated with the addition of small volumes of enzyme or substrate solution through the septum with a gas-tight glass syringe. Dissolved O_2 concentrations were continuously monitored inside the closed vials with fiber-optic oxygen minisensors and a FireSting meter (PyroScience GmbH) with automated pressure, humidity, and temperature correction. The fiber-optic minisensors are housed in stainless-steel needles (1.1 mm o.d.), with which the crimp vial septa can be pierced. Optical oxygen sensors were calibrated for maximum and minimum dissolved O_2 concentrations with air-equilibrated water and with a 300 mM Na_2SO_3 solution, respectively. Accurate temperature compensation was performed with optical temperature sensor spots (PyroScience GmbH) inside the vials. These sensor spots were regularly calibrated with the temperature probe of the FireSting meter.



With this type of enzyme assay, initial O_2 consumption rates were measured to determine K_m values for all enzymes with varying initial organic substrate concentrations, referred to as $K_m(S)$, except for cytochrome-*c* oxidase and kynurenine 3-monooxygenase (KMO) because of limited substrate availability. In addition, this type of enzyme assay was used to measure initial O_2 consumption rates in presence or absence of reaction products (see Appendix A for details). Inhibition of enzymatic activities due to the presence of reaction products (i.e., product inhibition) was tested for all enzymes, but only detected for KMO and laccase from *Trametes versicolor*, with 2,2'-azino-bis(3-ethylbenzothiazoline-6-sulfonic acid) diammonium salt (ABTS) as the substrate, at relevant product concentrations. Due to this observed product inhibition, K_m values with varying initial O_2 concentrations, referred to as $K_m(O_2)$, were determined as described for $K_m(S)$ above for KMO and laccase from *T. versicolor* with ABTS as the substrate (see Appendix A for details). Varying initial O_2 concentrations were achieved by mixing air-equilibrated buffer ($270 \pm 10 \mu M O_2$) with N_2 -purged buffer (approx. $0 \mu M O_2$) or O_2 -purged buffer ($1200 \pm 100 \mu M O_2$). For all other enzymes, $K_m(O_2)$ values were determined from complete O_2 consumption experiments performed with the same type of enzyme assay either in air-equilibrated or O_2 -purged buffer.

2.3 Enzyme assays for ^{18}O -KIEs and λ values

Enzyme assays to determine ^{18}O -KIEs and λ values were performed in air-equilibrated buffer solutions with saturating concentrations of all other substrates (see Appendix A for details). As saturating substrate concentrations, we considered either 10 times the $K_m(S)$ value or a sufficiently high substrate concentration to limit the difference between the initial and final reaction rate (v , determined with Eq. (8) and the corresponding $K_m(S)$ value) in the experiment to below 5 %. These enzyme assays were typically conducted in a 50 mL gas-tight glass syringe equipped with an optical oxygen sensor spot (PyroScience GmbH), an optical temperature sensor spot, and a small magnetic stir bar. Optical sensor spots were placed on the inside wall of the syringe, as close to the Luer-Lock tip as possible, and calibrated as described above for the fiber-optic oxygen sensors. These sensor spots allowed for a continuous, temperature-corrected measurement of O_2 concentrations through the glass wall via an optical fiber. The syringe was filled completely with a buffer solution containing all required substrates. To start the reaction, a small volume of enzyme solution was added through the Luer-Lock tip with a gas-tight glass syringe. Immediately after enzyme addition, a stainless-steel needle (0.8 mm o.d.) was attached to the Luer-Lock tip. To limit exchange of O_2 with the atmosphere, the needle was flushed with a few drops of assay solution and then pushed into a 12 mm thick chlorobutyl stopper. For experiments with diamine oxidase, the reaction was initiated by adding a small volume of substrate solution to assay solutions already containing the enzyme. Except during sampling, the syringe was placed on a magnetic stirring plate. Six sampling time-points (t_1 - t_6) were determined from the continuously monitored O_2 concentrations, typically at 200, 150, 120, 90, 70, and 50 μM remaining O_2 , corresponding to approx. 25-80 % O_2 consumption. To sample, the needle was removed from the stopper and the first mL assay solution was discarded. The next 3-7 mL (depending on O_2 concentration) were injected into 12 mL Exetainers (Labco Limited). Before starting an enzyme assay, Exetainers were closed with chlorobutyl septa, purged with He gas for 1 hour, and amended with 100-200 μL of 2 M NaOH or 2-3 M HCl, to stop enzymatic reactions in the added sample. To ensure equal headspace pressure in the Exetainers despite different sample volumes, Exetainer septa were



pierced with a stainless-steel needle (0.45 mm o.d.) connected with a T-piece to a slow He flow, and an open outlet submerged under 10 cm of water during sample injection. After sample injection, Exetainers were shaken and stored upside down until isotope analysis (see section 2.3). Procedural blanks were prepared by transferring 1-7 mL N₂-purged water with a 50 mL gas-tight glass syringe from closed, over-pressured serum bottles into He-purged Exetainers containing NaOH or HCl solution, as described above for enzyme assay samples. Similarly, quantification standards (see section 2.3 for details) were prepared by transferring 1-5 mL air-equilibrated water with a 50 mL gas-tight glass syringe into He-purged Exetainers. For each experiment, one or more control samples were prepared by transferring 3 mL leftover assay solution without enzyme with a 10 mL gas-tight glass syringe into a He-purged Exetainer containing NaOH or HCl solution. These control samples were used to determine the concentration and isotopic composition of O₂ at the start of the experiments (t₀).

Some enzyme assays with choline, diamine, and glucose oxidase were also performed in 4-10 identically prepared 12 mL crimp-top vials per assay, as described recently (de Carvalho et al., (2024)). Reactions were initiated by injecting a small volume of enzyme or substrate solution through the septa into filled vials. Prior to sampling, a fiber-optic oxygen microsensor (PyroScience GmbH) housed in a stainless-steel needle (0.5 mm o.d.) was inserted through the septa into the vials to measure the remaining O₂ concentration. The oxygen sensor was calibrated as described above. After initiating the reaction and before measuring O₂ concentrations, vials were shaken vigorously. To stop reactions at the desired degrees of O₂ consumption, 3-7 mL assay solution was transferred into He-purged Exetainers that had been amended with 100-200 µL 2 M NaOH or 2-3 M HCl. Procedural blanks, control samples, and quantification standards were prepared as described above. Experiments with diamine, choline and glucose oxidase performed with the two different setups resulted in equal ¹⁸O-KIEs and λ values, respectively, within error.

All samples, blanks, quantification standards, and controls were placed upside down on an orbital shaker at 125 rpm for 1 h, prior to analysis by gas chromatography coupled to isotope ratio mass spectrometry (GC-IRMS).

2.4 Stable isotope analysis of O₂

δ¹⁸O and δ¹⁷O values of O₂ were measured in the headspace of Exetainers with a GasBench II coupled via a ConFlo IV to a Delta V Plus isotope-ratio mass spectrometer (Thermo Fisher Scientific) as described recently (de Carvalho et al., 2024) and reported as permil (‰ ± one standard deviation) deviation relative to the international measurement standard Vienna Standard Mean Ocean Water (VSMOW) according to Eq. (5),

$$\delta^h\text{O} = \left(\frac{(^h\text{O}/^l\text{O})_{\text{sample}}}{(^h\text{O}/^l\text{O})_{\text{VSMOW}}} - 1 \right) \quad (5)$$

where (^hO/^lO)_{sample} is the ratio of heavy (¹⁸O or ¹⁷O) to light (¹⁶O) isotopes in O₂ in a sample and (^hO/^lO)_{VSMOW} is the ratio of heavy to light O isotopes in VSMOW. Briefly, seven 100 µL injections were made from each Exetainer headspace onto a 60 m Rt-Molsieve 5 Å PLOT column (Restek from BGB Analytik, 0.32 mm ID, 30 µm film thickness) kept at 25°C. Each



GC/IRMS sequence consisted of 5-14 samples from enzyme assays, 10-12 procedural blanks, 5 quantification standards, and 3 air standards. Half of the blanks were measured at the beginning of the sequence, the other half at the end. Air standards were evenly distributed across the sequence and consisted of 150 μL ambient air in 12 mL He. Air standards were used to verify instrument drift (which was never observed), and to perform a one-point calibration of the δ values to the VSMOW scale. The $\delta^{18}\text{O}$ and $\delta^{17}\text{O}$ values of O_2 in air were assumed to be 23.8 ‰ and 12.1 ‰, respectively (Luz and Barkan 2011; Laskar et al. 2019; Wostbrock et al. 2020). We recently showed, that for $\delta^{18}\text{O}$ values, a one-point calibration is sufficient, while for $\delta^{17}\text{O}$ values an additional correction factor must be used (de Carvalho et al., 2024). Procedural blanks were used to correct the measured δ values for blank contributions (Pati et al., 2016). Quantification standards were used to relate IRMS peak amplitudes to dissolved O_2 concentrations, and to correct δ values for instrument linearity (change in δ values with signal size) (Werner and Brand 2001).

2.5 Data analysis

Initial O_2 consumption rates were determined through linear regressions of the continuously measured O_2 concentrations versus time during the initial, linear phase of enzyme assays. ^{18}O -KIEs and λ values were obtained from a single linear regression of all O_2 isotope and concentration data from duplicate or triplicate enzyme assays according to Eqs. (6) and (7), respectively.

$$\ln\left(\frac{\delta^{18}\text{O} + 1}{\delta^{18}\text{O}_0 + 1}\right) = \left(\frac{1}{^{18}\text{O-KIE}} - 1\right) \cdot \ln\left(\frac{[\text{O}_2]}{[\text{O}_2]_0}\right) \quad (6)$$

$$\ln(\delta^{17}\text{O} + 1) = \lambda \cdot \ln(\delta^{18}\text{O} + 1) \quad (7)$$

where $[\text{O}_2]_0$ and $\delta^{18}\text{O}_0$ are the initial concentration and $\delta^{18}\text{O}$ value of O_2 , respectively, measured in the control sample (see section 2.2), and $[\text{O}_2]$, $\delta^{18}\text{O}$, and $\delta^{17}\text{O}$ are the values measured in each enzyme assay sample at the different time points. All linear regressions were performed with Microsoft Excel, and errors are reported as 95 % confidence intervals. K_m values were determined with a non-linear least square regression according to Eq. (8),

$$v_t = \frac{v_{\max} \cdot [i]_t}{K_m(i) + [i]_t} \quad (8)$$

where v_t is the O_2 consumption rate at a given time point t , v_{\max} is the maximum O_2 consumption rate of an enzymatic reaction, $[i]_t$ is the concentration of an organic substrate (S) or O_2 at time t , and $K_m(i)$ is the Michaelis constant determined under constant initial O_2 and variable initial substrate concentration ($K_m(\text{S})$), or under constant initial substrate and variable initial O_2 concentration ($K_m(\text{O}_2)$). For all $K_m(\text{S})$, as well as for $K_m(\text{O}_2)$ values determined for KMO and laccase from *T. versicolor* with ABTS, regressions were performed with initial rates of O_2 consumption (v_0) from different experiments against the nominal initial organic substrate concentrations ($[\text{S}]_0$), or against the measured initial O_2 concentrations ($[\text{O}_2]_0$), respectively. For all



other enzymes, where product inhibition was not detected, we determined $K_m(\text{O}_2)$ values from the continuous measurement of O_2 concentration over time ($[\text{O}_2]_t$) in a single enzyme assay, as described previously (Pati et al. 2022). For each time-point, v_t was calculated as the derivative of the measured $[\text{O}_2]_t$ vs. t (i.e., $\Delta[\text{O}_2]_t/\Delta t$) with Igor Pro software (WaveMetrics, Inc.). K_m values and corresponding 95 % confidence intervals were determined with R software (R Core Team 2023) using the MASS package (Venables and Ripley 2002).

3 Results

3.1 Kynurenine 3-monooxygenase

The flavin-dependent KMO was studied as an example for flavin monooxygenases, for which O_2 reduction mechanisms have been well-described. $K_m(\text{S})$ values for the native substrate L-kynurenine (0.012 ± 0.003 mM) and the co-substrate NADPH (0.009 ± 0.001 mM) were obtained from literature (Crozier and Moran 2007). $K_m(\text{O}_2)$ and ^{18}O -KIE were determined in experiments at optimal pH (7.5) and room temperature (23 ± 1 °C), with saturating concentrations (see section 2.2 for details) of L-kynurenine (1 mM) and NADPH (0.5 mM), as well as 2 mM dithiothreitol to prevent loss of KMO activity (Crozier and Moran 2007). A $K_m(\text{O}_2)$ of 6 ± 4 μM was determined from initial rates of O_2 consumption measured in 10 separate experiments with different initial O_2 concentrations (25-260 μM) as shown in Fig. 1A. The ^{18}O -KIE and λ values were determined from the change in concentration, $\delta^{18}\text{O}$, and $\delta^{17}\text{O}$ of O_2 over time, measured in duplicate experiments. Figs. 1B and 1C illustrate typical $\delta^{18}\text{O}$ data from one experiment. The combined data from both experiments (see section 2.4 for details) resulted in a ^{18}O -KIE of 1.0304 ± 0.0003 and a λ value of 0.545 ± 0.005 .

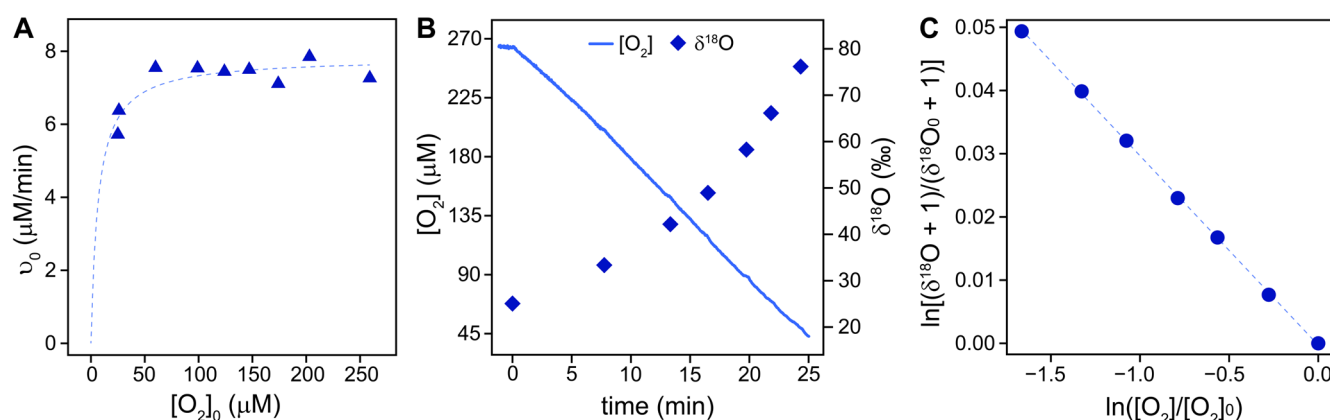


Figure 1. A) Initial rates of O_2 consumption (v_0) by KMO (blue triangles) measured in 10 separate experiments with different initial O_2 concentrations ($[\text{O}_2]_0$). The dotted line illustrates a non-linear least square regression fit according to Eq. (8), which was used to obtain $K_m(\text{O}_2)$. B) Continuously measured O_2 concentrations (solid blue line) and $\delta^{18}\text{O}$ values of O_2 measured in discrete samples (blue diamonds) over time during an experiment with KMO. C) Linearized and normalized data ($\delta^{18}\text{O}$ vs. $[\text{O}_2]$) from Fig. 1B, where $[\text{O}_2]_0$ and $\delta^{18}\text{O}_0$ represent the concentration and $\delta^{18}\text{O}$ value of O_2 at the beginning of the experiment. The dotted line shows a linear regression fit according to Eq. (6), from which the ^{18}O -KIE was obtained.



3.2 Flavin-dependent oxidases

290 Nine flavin-dependent oxidases were investigated. All of them convert O_2 to H_2O_2 in the oxidative half-reaction and oxidize
an organic substrate in the reductive half-reaction. Pyruvate oxidase was the only flavin-dependent oxidase that required
cofactors for activity, namely thiamine diphosphate, $MnSO_4$, and FAD. Experiments with cholesterol oxidase were performed
with the surfactant Thesit® and isopropanol due to the low water solubility of the native substrate cholesterol. Experiments
with glucose and alcohol oxidase were each performed with their native and an alternative substrate: Glucose and mannose, in
295 the case of glucose oxidase, and methanol and ethanol, the case of alcohol oxidase. Experiments to determine ^{18}O -KIEs for
alcohol, choline, and L-lysine oxidase were performed at two different initial O_2 concentrations ($260 \pm 10 \mu M$ and 1200 ± 100
 μM).

3.2.1 Michaelis constants for organic substrates

$K_m(S)$ values were determined at $260 \pm 10 \mu M$ initial O_2 concentration, as described for the $K_m(O_2)$ value of KMO (see section
300 3.1). However, initial rates of O_2 consumption were measured at different initial organic substrate concentrations. For all
flavin-dependent oxidases, except pyruvate oxidase, $K_m(S)$ values were determined for the native substrate, with values ranging
from $0.011 \pm 0.004 \text{ mM}$ for L-lysine oxidase to $36 \pm 18 \text{ mM}$ for glucose oxidase (see Table 2). The $K_m(S)$ for pyruvate oxidase
could not be determined as the initial rates of O_2 consumption were not linear across all relevant pyruvate concentrations. For
alcohol oxidase, the alternative substrate ethanol had a substantially higher $K_m(S)$ than the native substrate methanol (22 ± 6
305 vs. $0.6 \pm 0.4 \text{ mM}$). For D-mannose, the alternative substrate of glucose oxidase, a $K_m(S)$ could not be determined because
initial rates of O_2 consumption increased linearly with D-mannose concentrations up to the solubility limit of D-mannose.



Table 2. $K_m(S)$, $K_m(O_2)$, ^{18}O -KIEs and λ values determined for all enzymes investigated in this study with errors given as 95 % confidence intervals.

Active site	Enzyme	Substrate	$K_m(S)$ (mM)	$K_m(O_2)$ (μ M)	^{18}O -KIE (-)	λ (-)
Flavin	kynurenine 3-monooxygenase	L-kynurenine	n.d. ^a	6 ± 4	1.0304 ± 0.0003	0.545 ± 0.005
Flavin	alcohol oxidase	methanol	0.6 ± 0.4	1017 ± 93	1.028 ± 0.001	0.491 ± 0.008
Flavin	alcohol oxidase	ethanol	22 ± 6	901 ± 200	1.0276 ± 0.0007	0.483 ± 0.007
Flavin	cholesterol oxidase	cholesterol	0.3 ± 0.2	271 ± 12	1.0191 ± 0.0003	0.53 ± 0.01
Flavin	choline oxidase	choline	0.5 ± 0.1	312 ± 21	1.0194 ± 0.0006	0.537 ± 0.008
Flavin	D-amino acid oxidase	D-alanine	2.3 ± 0.4	92 ± 7	1.0509 ± 0.0008	0.546 ± 0.004
Flavin	glucose oxidase	D-glucose	36 ± 18	116 ± 14	1.029 ± 0.001	0.523 ± 0.009
Flavin	glucose oxidase	D-mannose	n.d. ^a	3.9 ± 0.5	1.0341 ± 0.0005	0.536 ± 0.004
Flavin	L-lactate oxidase	L-lactate	0.3 ± 0.1	80 ± 3	1.044 ± 0.001	0.540 ± 0.006
Flavin	L-lysine oxidase	L-lysine	0.011 ± 0.004	1291 ± 73	1.046 ± 0.001	0.543 ± 0.004
Flavin	pyruvate oxidase	pyruvate	n.d. ^a	225 ± 16 ^b	1.0565 ± 0.0009	0.547 ± 0.002
Flavin	sarcosine oxidase	sarcosine	8 ± 3	83 ± 3	1.047 ± 0.001	0.536 ± 0.007
Copper	L-ascorbate oxidase	L-ascorbic acid	0.14 ± 0.05	144 ± 11	1.0086 ± 0.0006	0.54 ± 0.01
Copper	bilirubin oxidase	bilirubin	0.018 ± 0.009	73 ± 3	1.0222 ± 0.0005	0.535 ± 0.009
Copper	diamine oxidase	histamine	0.018 ± 0.007	9.4 ± 0.5	1.0103 ± 0.0007	0.51 ± 0.03
Copper	laccase from <i>A. bisporus</i>	hydroquinone	2 ± 3	36 ± 2	1.0190 ± 0.0002	0.530 ± 0.007
Copper	laccase from <i>T. versicolor</i>	hydroquinone	0.23 ± 0.04	72 ± 4	1.0196 ± 0.0007	0.539 ± 0.007
Copper	laccase from <i>T. versicolor</i>	ABTS	0.12 ± 0.07	47 ± 59	1.0194 ± 0.0005	0.54 ± 0.01
copper/ heme	cytochrome-c oxidase	cytochrome c	n.d. ^a	3.3 ± 0.5	1.0189 ± 0.0005	0.543 ± 0.009

^a not determined

^b tentative value (see section 3.2.2)



3.2.2 Michaelis constants for O₂

K_m(O₂) values were determined from complete O₂ consumption experiments at saturating organic substrate concentrations (see section 2.2), as shown in Figs. 2A and 2B for L-lactate oxidase as an example. Three flavin-dependent oxidases exhibited K_m(O₂) values exceeding air-saturated O₂ concentrations in the presence of their native substrates, namely alcohol oxidase with both substrates (1017 ± 93 μM and 901 ± 200 μM), choline oxidase (312 ± 21 μM), and L-lysine oxidase (1291 ± 73 μM). For these enzymes, K_m(O₂) values were obtained from complete O₂ consumption experiments with initial O₂ concentrations of 1200 ± 100 μM. The remaining flavin-dependent oxidases displayed K_m(O₂) values between 80 ± 3 μM and 260 ± 12 μM (see Table 2). The K_m(O₂) value determined for pyruvate oxidase (225 ± 16 μM) should be considered a tentative value as the effect of product inhibition could not be assessed, and the K_m(S) could not be determined. K_m(O₂) values for alcohol and glucose oxidase were also determined at saturating concentrations of the alternative substrates, ethanol and D-mannose, respectively. In the case of alcohol oxidase, the K_m(O₂) values determined with methanol (1017 ± 93 μM) and ethanol (901 ± 200 μM) as substrates were equal within error. In contrast, glucose oxidase exhibited a significantly lower K_m(O₂) value with D-mannose as the substrate (3.9 ± 0.5 μM) compared to the value determined with the native substrate D-glucose (116 ± 14 μM).

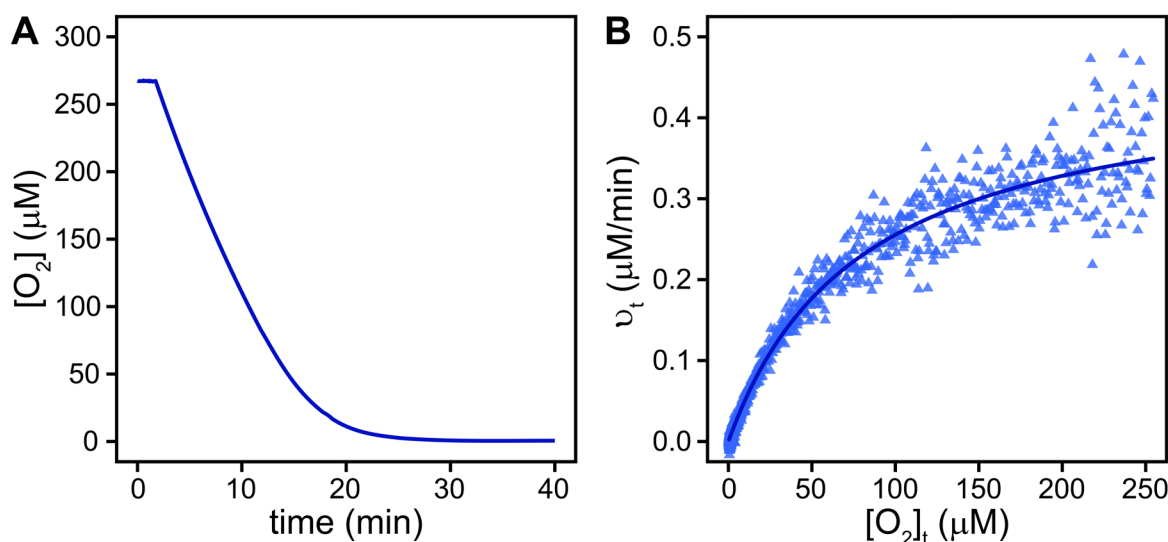


Figure 2. A) O₂ concentration ([O₂]) over time in a complete O₂ consumption experiment with L-lactate oxidase. B) Blue triangles show reactions rates (v_t), derived by differentiating the data in Fig. 2A at corresponding O₂ concentrations ([O₂]_t). The solid line shows a non-linear least square regression fit according to Eq. (8).



3.2.3 ^{18}O -Kinetic isotope effects and λ values

All ^{18}O -KIEs were determined in air-saturated buffer solutions with saturating native substrate concentrations, as described for KMO (see section 3.1). The ^{18}O -KIEs of D-amino-acid, L-lactate, L-lysine, pyruvate, and sarcosine oxidase ranged from 1.044 \pm 0.001 to 1.0565 \pm 0.0009 (see Table 2). In contrast, alcohol, cholesterol, choline, and glucose oxidase were associated with lower ^{18}O -KIEs, ranging from 1.0191 \pm 0.0003 to 1.029 \pm 0.001 (see Table 2). Because alcohol, choline, and L-lysine oxidase exhibited $K_m(\text{O}_2)$ values above air-saturation, their ^{18}O -KIEs were additionally determined in O_2 -purged buffer with initial O_2 concentrations of 1200 \pm 100 μM (see Appendix B for details). For all three enzymes, the ^{18}O -KIEs were identical, within error, irrespective of the initial O_2 concentration (data not shown). The ^{18}O -KIEs of alcohol oxidase with the two substrates methanol and ethanol were also identical within error (see Table 2). However, the ^{18}O -KIE determined for glucose oxidase with D-mannose was larger (1.0341 \pm 0.0005) than that determined with D-glucose (1.029 \pm 0.001). λ values ranged between 0.523 \pm 0.009 and 0.547 \pm 0.002 (see Table 2) for all flavin oxidases except for alcohol oxidase, which yielded lower λ values of 0.491 \pm 0.008 and 0.483 \pm 0.007 with methanol and ethanol, respectively.

3.3 Copper-dependent oxidases

Five copper-dependent oxidases were investigated. Namely, Laccases, L-ascorbate oxidase, and bilirubin oxidase, which convert O_2 to water in the oxidative half-reaction, and diamine oxidase, which converts O_2 to H_2O_2 . All experiments were performed with native substrates, except experiments with laccase (see below), in a buffered, air-equilibrated solution at optimal pH and room temperature.

Laccases are multicopper oxidases that can oxidize a wide variety of substrates and lack a specific native substrate (Strong and Claus 2011). Hydroquinone and ABTS were selected as substrates in this study because they displayed different substrate-to- O_2 consumption stoichiometries. Four ABTS molecules are required to reduce one molecule of O_2 , while only two hydroquinone molecules are required to reduce one molecule of O_2 (see Appendix C). Despite these differences, laccase from *T. versicolor* yielded similar values for $K_m(\text{S})$, $K_m(\text{O}_2)$, and ^{18}O -KIEs irrespective of the substrate oxidized. With hydroquinone as the substrate, $K_m(\text{S})$, $K_m(\text{O}_2)$, and ^{18}O -KIE were 0.23 \pm 0.04 mM, 72 \pm 4 μM , and 1.0196 \pm 0.0007, respectively. With ABTS as the substrate, $K_m(\text{S})$, $K_m(\text{O}_2)$, and ^{18}O -KIE were 0.12 \pm 0.07 mM, 47 \pm 59 μM , and 1.0194 \pm 0.0005, respectively. Laccase from *Agaricus bisporus* exhibited a 10-fold higher $K_m(\text{S})$ and a 2-fold lower $K_m(\text{O}_2)$ with hydroquinone as the substrate compared to laccase from *T. versicolor* under identical conditions (see Table 2). However, the ^{18}O -KIEs were identical within error (1.0190 \pm 0.0002) and λ values ranged from 0.530 \pm 0.007 to 0.54 \pm 0.01 (see Table 2).

The remaining three copper-dependent oxidases, L-ascorbate, bilirubin, and diamine oxidase displayed low $K_m(\text{S})$ values between 0.14 \pm 0.05 mM and 0.018 \pm 0.007 mM (see Table 2). $K_m(\text{O}_2)$ values decreased from 144 \pm 11 μM for L-ascorbate oxidase to 73 \pm 3 μM for bilirubin oxidase and 9.4 \pm 0.5 μM for diamine oxidase. L-Ascorbate and diamine oxidase exhibited the lowest observed ^{18}O -KIEs of all enzymes in this study with 1.0086 \pm 1.0006 and 1.0103 \pm 0.0007, respectively, while bilirubin oxidase had an ^{18}O -KIE of 1.0223 \pm 1.0005. λ values ranged from 0.51 \pm 0.03 to 0.54 \pm 0.01 (see Table 2).



During experimental assays with diamine oxidase, O₂ production due to catalase contamination in the lyophilized diamine
oxidase powder was detected. Catalase catalyzes the oxidation of H₂O₂ to H₂O and O₂, which could lead to inaccurate
measurements of O₂ consumption by diamine oxidase. To address this potential interference, ¹⁸O-KIEs for diamine oxidase
were determined in the presence of the catalase contamination alone and with the addition of excess horseradish peroxidase
and ascorbic acid. Horseradish peroxidase catalyzes the oxidation of H₂O₂ and ascorbic acid to H₂O and dehydroascorbic
acid. In the presence of excess horseradish peroxidase, H₂O₂ was converted to H₂O faster than catalase could reduce H₂O₂ to
H₂O and O₂. The ¹⁸O-KIEs determined for diamine oxidase were found to be identical within error, regardless of catalase
activity (data not shown).

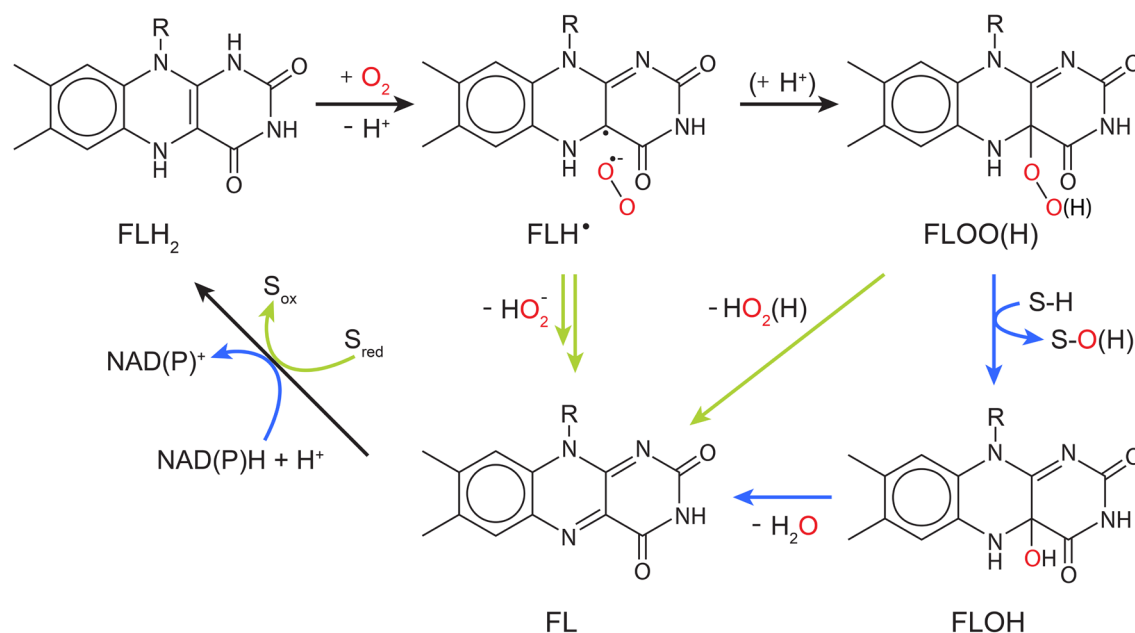
3.4 Cytochrome-*c* oxidase

Cytochrome-*c* oxidase is a heme-copper dependent-oxidase, in which the heme *a*₃ subunit initially binds O₂ (Yoshikawa and
Shimada 2015). The K_m(S) was not determined, but all experiments were performed with 25 μM cytochrome *c* and 3 mM
ascorbic acid, to continuously reduce the product ferricytochrome *c* back to the substrate ferrocycytochrome *c*. K_m(S) values for
ferrocycytochrome *c* are reported to be 1.48 μM or lower (Merle and Kadenbach 1982). Therefore, the 25 μM of cytochrome *c*
used is considered a saturating substrate concentration. The K_m(O₂) was 3.3 ± 0.5 μM, the ¹⁸O-KIE was 1.0189 ± 0.0005, and
the λ value was 0.543 ± 0.009 (see Table 2).

4 Discussion

4.1 ¹⁸O-KIEs of flavin-dependent O₂-consuming enzymes

Flavin-dependent O₂-consuming enzymes utilize derivatives of the vitamin riboflavin as cofactors in their active sites. The
organic flavin cofactor can be present in three different redox states: fully oxidized flavin (FL), radical flavin intermediate
(FLH[•]), and fully reduced flavin (FLH₂ or FLH⁻). The oxidation of FLH₂ to FL releases two electrons and two protons, which
can be used for the reduction of O₂ (Massey 2002), as illustrated in a simplified catalytic cycle in Fig. 3. The reduction of O₂
by both flavin-dependent monooxygenases and oxidases starts with an outer-sphere single-electron transfer from FLH₂ (or
FLH⁻) to O₂ forming FLH[•] and O₂^{-•}. A recombination of the two radical species then forms a peroxyflavin intermediate (FLOO⁻),
which can be protonated to a hydroperoxyflavin intermediate (FLOOH). In all known flavin-dependent monooxygenases,
the (hydro)peroxyflavin can be detected and is responsible for substrate hydroxylation with concomitant O-O bond cleavage
to form a hydroxyflavin (FLOH) (Massey 2002) (see blue arrows in Fig. 3). In a subsequent step, FLOH reacts to FL by
releasing H₂O (see blue arrows in Fig. 3). In flavin-dependent oxidases, FLOO(H) has not been observed directly, and its
formation remains a matter of ongoing debate (Massey 2002). In addition to FL formation similar to the monooxygenation
pathway (FLH[•] and O₂^{-•} recombination to FLOO(H) and subsequent release of hydrogen peroxide), FL can also be formed
through a sequence of outer-sphere electron and proton transfer steps from FLH[•] to O₂^{-•} without covalent-bond formation
between the flavin and O₂ (see green arrows in Fig. 3) (Massey 2002; Mattevi 2006; Chaiyen et al. 2012). The reduction of FL



390 **Figure 3. O₂ reduction mechanism of flavin-dependent oxidases and monooxygenases. Black arrows indicate common reaction steps, blue arrows indicate reaction steps performed by monooxygenases, and green arrows indicate reaction steps performed by oxidases. S represents the organic substrate.**

to FLH₂ is coupled with substrate or co-substrate oxidation in oxidases and monooxygenases, respectively, to complete the catalytic cycle (see Fig. 3).

395 In this study, we determined the first ¹⁸O-KIE for a flavin-dependent monooxygenase, namely KMO, which was 1.0305 ± 0.0003. The magnitude of this isotope effect indicates that changes in bond order of O₂ occur during the rate-limiting step of the reaction between KMO and O₂, excluding O₂ binding and product release as possible rate-limiting steps. Hence, the rate-limiting reaction step of KMO is the formation of O₂^{•-}, FLOO^{•-}, FLOOH, or S-OH and FLOH (see blue arrows in Fig. 3). ¹⁸O-EIEs have been calculated for the reversible formation of O₂^{•-}, HO₂⁻, H₂O₂, and two H₂O from O₂ as 1.033, 1.034, 1.009, and 0.968, respectively (Roth and Klinman 2005). When comparing experimental ¹⁸O-KIEs to calculated ¹⁸O-EIEs, it is generally assumed that a measured ¹⁸O-KIE (i) reflects intrinsic ¹⁸O-KIEs of all electron and proton transfer steps up to, and including, the rate-limiting step and (ii) is similar to, but not larger than, the ¹⁸O-EIE calculated for the formation of the product/intermediate after the rate-limiting step (Roth and Klinman 2005). Based on these ¹⁸O-EIEs, the reduction of O₂ by KMO is thus likely characterized by a rate-limiting O₂^{•-} or FLOO^{•-} formation. However, this conclusion conflicts with studies suggesting that substrate hydroxylation is the rate-limiting step (Özkılıç and Tüzün 2019).

405 Similar magnitudes of ¹⁸O-KIEs compared to KMO have been determined in this study for glucose oxidase: 1.029 ± 0.001 and 1.0341 ± 0.0005 with D-glucose and D-mannose as the substrate, respectively. These values agree with previous studies of the same enzyme (Su and Klinman 1998). Based on ¹⁸O-EIEs, solvent isotope effects, and viscosity effects, Roth and Klinman, (2003) suggested the initial outer sphere electron transfer from FLH^{•-} to O₂ to be the rate-limiting step of O₂



410 reduction by glucose oxidase. The ^{18}O -KIEs determined for cholesterol, choline, and alcohol oxidase in this study were similar to, or lower than, those determined for KMO and glucose oxidase (1.0191-1.028, see Table 2). Because these isotope effects were still larger than the calculated ^{18}O -EIE for H_2O_2 or H_2O formation (1.009, and 0.968, respectively), these enzymes likely also have a rate-limiting $\text{O}_2^{\cdot-}$ or $\text{FLOO}^{\cdot-}$ formation. In contrast, D-amino-acid, L-lactate, L-lysine, pyruvate, and sarcosine oxidase exhibited much larger ^{18}O -KIEs (1.044-1.0565, see Table 2). These distinctively high ^{18}O -KIEs clearly suggest a
415 different rate-limiting step than previously discussed, even though the first outer-sphere electron transfer to O_2 has also been proposed as the rate-limiting step for D-amino-acid oxidase (Kiss and Ferenczy 2019). To date, ^{18}O -KIEs of this magnitude have only been measured for L-amino acid (1.0478) and D-amino-acid oxidase (1.053) by Cheah et al. (2014). The only ^{18}O -EIE of similar magnitude was calculated for the formation of O_2^{2-} , a two-electron reduction product of O_2 , with a value of 1.050 (Roth and Klinman 2003).

420 Considering the two possible reaction mechanisms described in Fig. 3 for flavin-dependent oxidases, we suggest that glucose, cholesterol, choline, and alcohol oxidase, like KMO, reduce O_2 through the formation of $\text{FLOO}(\text{H})$ with a rate-limiting formation of either $\text{O}_2^{\cdot-}$ or $\text{FLOO}^{\cdot-}$. The same applies to glycolate oxidase with a ^{18}O -KIE of 1.023 (Guy et al., 1993; Ribas-Carbo et al., 1995; Cheah et al., 2014). However, for D-amino-acid, L-amino-acid, L-lactate, L-lysine, pyruvate, and sarcosine oxidase we suggest the alternative O_2 reduction mechanism, where FL is formed directly from $\text{FLH}^{\cdot+}$ and $\text{O}_2^{\cdot-}$ without the
425 formation of $\text{FLOO}(\text{H})$ (see green arrows in Fig. 3). Still, the exact nature of the rate-limiting step (a second single electron transfer, a proton-coupled electron transfer, or a hydrogen atom transfer) in this alternative O_2 reduction mechanism cannot be inferred from the current experimental evidence. It is also possible that the rate-limiting step differs among the six oxidases with ^{18}O -KIEs between 1.044 and 1.057, or that the first electron transfer to O_2 is partially rate-limiting in some of these enzymes, which could explain the lower-than-expected ^{18}O -KIEs for such a rate-limiting step.

430 For KMO, cholesterol, choline, and glycolate oxidase, as well as glucose oxidase with 45 different substrates, which we consider to share a common reaction mechanism, we found a tentative correlation between ^{18}O -KIEs and the corresponding $K_m(\text{O}_2)$ values (see Fig. 4). The $K_m(\text{O}_2)$ values for glucose oxidase with the substrate 2-deoxy-D-glucose and for glycolate oxidase were reported to be $25 \pm 5 \mu\text{M}$ and $210 \mu\text{M}$, respectively (Macheroux et al. 1991; Roth and Klinman 2003). Based on the limited number of data points, we do not consider the correlation to be necessarily linear as shown in Fig. 4. However, the
435 data clearly indicates that enzymes with lower $K_m(\text{O}_2)$ values have higher ^{18}O -KIEs, ranging from choline oxidase with a $K_m(\text{O}_2)$ of $298 \pm 20 \mu\text{M}$ and a ^{18}O -KIE of 1.0194 ± 0.0006 , to glucose oxidase with D-mannose as the substrate with a $K_m(\text{O}_2)$ of $3.9 \pm 0.6 \mu\text{M}$ and a ^{18}O -KIE of 1.0341 ± 0.0005 . Since ^{18}O -KIEs reflect the ratios of reaction rates of the different O_2 isotopologues, a correlation between ^{18}O -KIE and $K_m(\text{O}_2)$ only makes sense when we consider the kinetic properties of the Michaelis constant. $K_m(\text{O}_2)$ is the ratio of the two apparent rate constants “ v_{max} ” and “ $v_{\text{max}}/K_m(\text{O}_2)$ ”. “ v_{max} ” represents the
440 observed rate at high substrate concentration and includes all steps after the formation of an enzyme-substrate complex (Northrop 1998). “ $v_{\text{max}}/K_m(\text{O}_2)$ ” represents the observed rate at low substrate concentration, encompassing all steps beginning with interaction of enzyme with O_2 up to, and including, the first rate-limiting step (Northrop 1998). In O_2 -consuming enzymes, O_2 typically binds to the enzyme after binding of the organic substrate (oxygenases), or in a ping-pong mechanism (oxidases)



(Malmstrom 1982; Romero et al. 2018). Thus, the only step covered by “ $v_{\max}/K_m(\text{O}_2)$ ” but not by “ v_{\max} ” is O_2 binding. Therefore, when $K_m(\text{O}_2)$ is very large, “ $v_{\max}/K_m(\text{O}_2)$ ” is much smaller than “ v_{\max} ”, and O_2 binding must be slower than the catalytic step. However, as $K_m(\text{O}_2)$ decreases, “ $v_{\max}/K_m(\text{O}_2)$ ” becomes closer to “ v_{\max} ”, and O_2 binding contributes less to the overall reaction rate. Consequently, $K_m(\text{O}_2)$ can be interpreted as a proxy for the extent to which O_2 binding contributes to the overall reaction rate. If O_2 binding was the sole rate-limiting step, an apparent ^{18}O -KIE close to 1 would be expected because no bond changes would occur in O_2 . However, this is not the case for any O_2 -consuming enzyme studied so far. On the other extreme, if O_2 binding does not contribute to the overall rate at all, the apparent ^{18}O -KIE is expected to reflect the intrinsic ^{18}O -KIE of the rate-limiting step. Accordingly, the intrinsic ^{18}O -KIE for the rate-limiting step of $\text{O}_2^{\cdot -}$ or FLOO^- formation is likely between 1.030 and 1.035, based on both calculated ^{18}O -EIEs for these reactions (1.033-1.034) (Roth and Klinman 2003), and on the maximum ^{18}O -KIEs observed for glucose oxidase (1.0341 ± 0.0005) and KMO (1.0304 ± 0.0003). The lower ^{18}O -KIEs (1.019-1.023), particularly for cholesterol, choline, and glycolate oxidase, can thus still arise from a rate-limiting $\text{O}_2^{\cdot -}$ or FLOO^- formation, but with increasing contributions from a slower O_2 binding to the overall reaction rate.

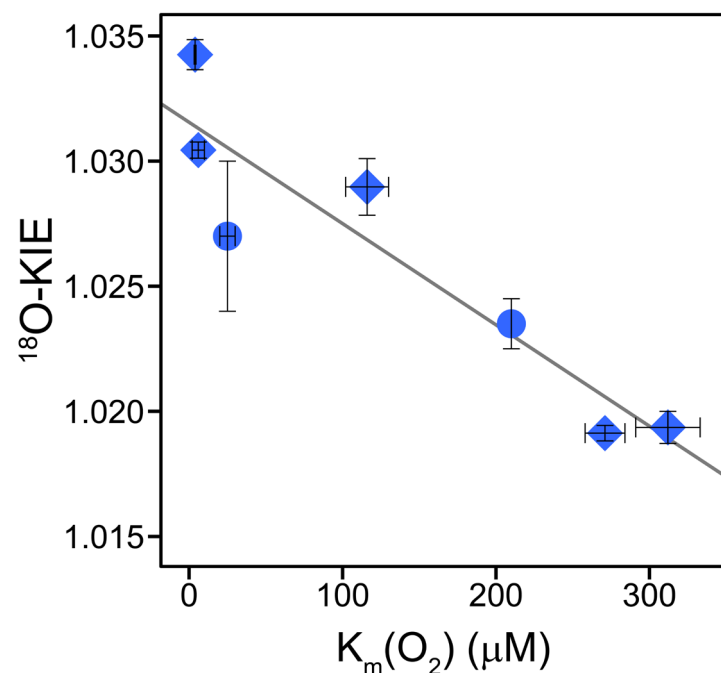


Figure 4. Correlation of ^{18}O -KIEs and corresponding $K_m(\text{O}_2)$ values of glucose, choline, cholesterol, and glycolate oxidase as well as KMO. Blue diamonds represent the ^{18}O -KIEs and corresponding $K_m(\text{O}_2)$ values determined in this study. Blue circles represent the ^{18}O -KIEs and corresponding $K_m(\text{O}_2)$ values obtained from literature for glycolate oxidase and for glucose oxidase with 2-deoxy-D-glucose as the substrate (Macheroux et al., 1991; Su and Klinman, 1999; Roth and Klinman, 2003; Cheah et al., 2014). Error bars indicate 95 % confidence intervals. The solid line indicates a tentative linear correlation.



Alcohol oxidase, with either methanol or ethanol as the substrate, was the only enzyme with ^{18}O -KIEs close to or below 1.03 that did not follow the observed trend between $K_m(\text{O}_2)$ values and ^{18}O -KIEs discussed above. $K_m(\text{O}_2)$ values of alcohol oxidase (1017 ± 93 and 901 ± 200) were substantially larger than $K_m(\text{O}_2)$ values of all other flavin-dependent enzymes studied, except for L-lysine oxidase, which likely has a different O_2 reduction mechanism (formation of O_2^{2-}). Interestingly, alcohol oxidase was the only enzyme tested in this study that exhibited particularly low λ values between 0.483 ± 0.007 and 0.488 ± 0.009 (see Table 2). These values are not only lower than typical λ values (0.51-0.53) but also significantly lower than λ values observed for all other enzymes in this study, which ranged from 0.51 ± 0.03 to 0.547 ± 0.002 (see Table 2). We note that λ values determined for the majority of enzymes in this study are close to, but slightly higher than previously determined λ values of 0.51 to 0.53 for biological O_2 consumption (Young et al. 2002; Luz and Barkan 2005; Ash et al. 2020; Hayles and Killingsworth 2022). It is possible that the applied $\delta^{17}\text{O}$ scale correction factor from de Carvalho et al., (2024) leads to a slight overestimation of λ values. Regardless of this uncertainty in the $\delta^{17}\text{O}$ scale correction factor, the λ values determined for alcohol oxidase are clearly much lower than any previously determined λ values for biological O_2 consumption, and significantly lower than those for any other enzyme studied here. This difference in λ values suggests a unique O_2 reduction mechanism for alcohol oxidase, differing from the mechanism proposed for enzymes that exhibit a correlation between ^{18}O -KIEs and $K_m(\text{O}_2)$ values. However, this reduction mechanism cannot be further elucidated in this study.

4.2 ^{18}O -KIEs of metal-dependent O_2 -consuming enzymes

Unlike flavin-dependent O_2 -consuming enzymes, which have a relatively conserved active site and catalytic mechanism, iron- and copper-dependent O_2 -consuming enzymes are known to employ a wide variety of different active site structures and catalytic mechanisms (Costas et al. 2004; Blank et al. 2010; Liu et al. 2014; Solomon et al. 2014; Huang and Groves 2018). For the five copper-dependent oxidases tested in this study and for six (out of seven) copper-dependent monooxygenases and oxidases examined in previous research, the ^{18}O -KIEs grouped closely around two main values. Namely, L-ascorbate and diamine oxidase from this study, as well as tyrosinase, bovine serum amine oxidase, and amine oxidase from *Hansenula polymorpha* were characterized by ^{18}O -KIEs between 1.0086 and 1.011 (see Tables 1 and S1 in the supplement) (Feldman et al. 1959; Su and Klinman 1998; Welford et al. 2007). Conversely, the ^{18}O -KIEs of bilirubin oxidase and the two laccases from this study, as well as peptidylglycine monooxygenase, dopamine β -monooxygenase, and galactose oxidase ranged between 1.0173 and 1.223 (see Tables 1 and S1 in the supplement) (Tian et al. 1994; Francisco et al. 2003; Humphreys et al. 2009). The only copper-dependent enzyme studied so far that fell in between these two clusters is pea-seedling amine oxidase with an ^{18}O -KIE of 1.014 ± 0.001 (Mukherjee et al. 2008). The two groups of copper-dependent enzymes defined by the two groups of ^{18}O -KIE values, both contain a mix of monooxygenases and oxidases (see Fig. 5). The monooxygenases peptidylglycine monooxygenase, dopamine β -monooxygenase, and tyrosinase catalyze the incorporation of one O atom from O_2 into their substrate. Multicopper oxidases, including laccase, L-ascorbate oxidase, and bilirubin oxidase, reduce O_2 to two H_2O . The cofactor-dependent mononuclear copper enzymes (copper amine oxidases including diamine oxidase and galactose oxidase)



495 reduce O_2 to H_2O_2 (Mure et al. 2002; Humphreys et al. 2009). Despite these differences, all copper-dependent O_2 -consuming enzymes form common copper-oxygen intermediates, namely copper-superoxo ($Cu(II)-OO^*$), copper-peroxo ($Cu(II)-OO^*$), and copper-hydroperoxo ($Cu(II)-OOH$) species. Figure 6 shows the electron and proton transfer steps involved in the formation of these intermediates. ^{18}O -EIEs for the reversible formation of these three copper-oxygen species have been determined to be 1.009-1.010 for copper-superoxo, 1.018-1.031 for copper-peroxo, and 1.025-1.026 for copper-hydroperoxo intermediates (Mukherjee et al., 2008; Humphreys et al., 2009). The copper-dependent enzymes that exhibited ^{18}O -KIEs between 1.0173 and 1.223 are thus likely characterized by a rate-limiting step involving the formation of a copper-peroxo or copper-hydroperoxo intermediate. Accordingly, studies of peptidylglycine and dopamine β -monooxygenase, which exhibited ^{18}O -KIEs of 1.0173 ± 0.0009 and 1.0197 ± 0.0003 , respectively, suggested a rate-limiting hydrogen atom abstraction by a copper-superoxo intermediate to form a copper-hydroperoxo species (Evans et al. 2003; Osborne and Klinman 2011). The ^{18}O -KIE of 1.019 ± 0.001 determined for galactose oxidase by Humphreys et al., (2009) was also attributed to a rate-limiting hydrogen atom abstraction by a copper-superoxo intermediate. The rate-limiting steps of multicopper oxidases, such as bilirubin oxidase and laccase, have not been firmly established. However, based on the ^{18}O -KIEs determined in this study, and the comparison with the three enzymes with similar ^{18}O -KIEs, a rate limiting copper-hydroperoxo formation by hydrogen atom abstraction seems likely. Similarly, the copper-dependent enzymes that displayed ^{18}O -KIEs between 1.0086 and 1.011 are likely characterized by a rate-limiting copper-superoxo formation, based on comparisons with ^{18}O -EIEs (1.009 - 1.010). Accordingly, copper-superoxo formation has been suggested as the rate-limiting step for bovine serum amine oxidase and amine oxidase from *H. polymorpha* (Su and Klinman 1998; Mills et al. 2002). It can thus be assumed that tyrosinase, as well as L-ascorbate and diamine oxidase also have a rate-limiting step involving the formation of a copper-superoxo intermediate. For pea-seedling amine oxidase, for which a ^{18}O -KIE of 1.014 ± 0.001 was determined (Mukherjee et al. 2008), a rate-limiting step involving copper-peroxo formation has also been proposed. However, the preceding copper-superoxo formation is partially rate-limiting, which acts to lower the observed ^{18}O -KIE value from the expected ^{18}O -EIE range of 1.018-1.031 (Mukherjee et al. 2008).

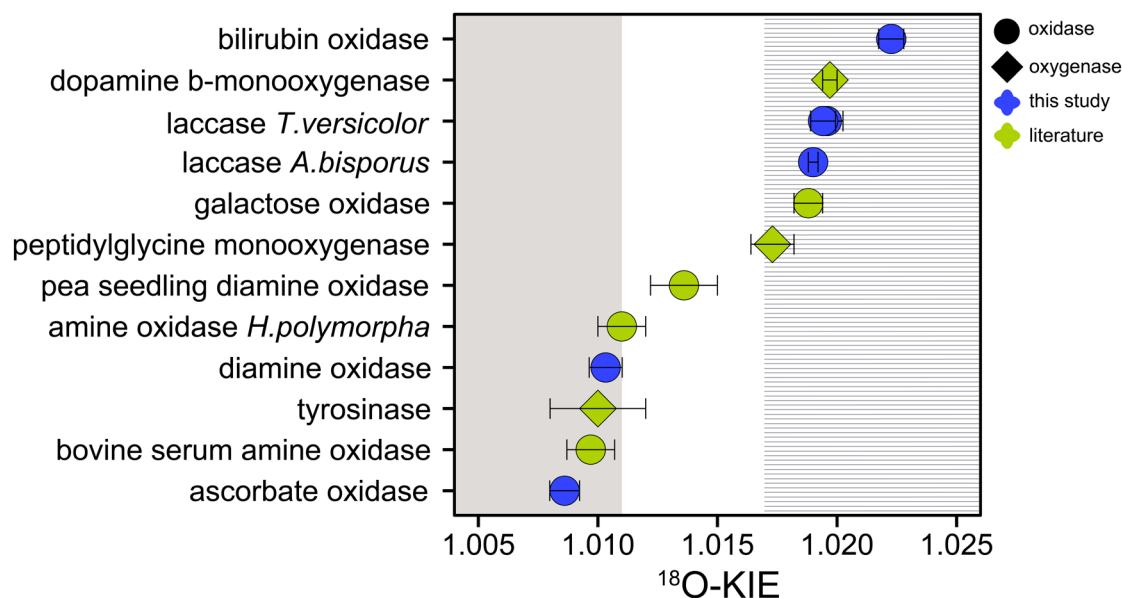


Figure 5. ^{18}O -KIEs for copper-dependent O_2 -consuming oxidases (circles) and monooxygenases (diamonds) reported in this (blue) and previous studies (green) (Feldman et al., 1959; Tian et al., 1994; Su and Klinman, 1998; Francisco et al., 2003; Welford et al., 2007; Mukherjee et al., 2008; Humphreys et al., 2009). Error bars indicate 95 % confidence intervals or standard deviations. Grey and dashed areas represent expected ^{18}O -KIE ranges for a rate-limiting copper-superoxo formation (grey area), and hydrogen atom abstraction by a copper-superoxo species (dashed area) (Mukherjee et al., 2008; Humphreys et al., 2009).

The ^{18}O -KIE of 1.0189 ± 0.0005 determined here for cytochrome-*c* oxidase is consistent with previous reports from the literature (Ribas-Carbo et al. 1995; Cheah et al. 2014). Cytochrome-*c* oxidase is a hetero di-nuclear copper-heme oxidase, in which a copper and a heme-iron are involved in the O_2 -reduction mechanism (Yoshikawa and Shimada 2015). Iron-dependent enzymes form similar reactive oxygen intermediates, as described above for copper-dependent enzymes, including iron-superoxo ($\text{Fe(III)-OO}^{\bullet}$) and iron-hydroperoxo (Fe(III)-OOH) intermediates (see Fig. 6). In addition, iron can be oxidized further in certain active site structures to a high-valent iron-oxo (Fe(IV)=O) intermediate. The calculated ^{18}O -EIEs are also similar in magnitude, with 1.008-1.009 for iron-superoxo formation, 1.014-1.017 for iron-hydroperoxo formation, and 1.029 for iron-oxo formation (Mirica et al. 2008). Previous studies have determined ^{18}O -KIEs for 12 iron-dependent O_2 -consuming enzymes showing a continuous range from 1.009 ± 0.001 for soybean lipoxygenase (Guy et al. 1992), to 1.0281 ± 0.0004 for alternative oxidase (Cheah et al. 2014). Observed ^{18}O -KIEs for iron-dependent enzymes have consistently reflected the intrinsic ^{18}O -KIE of the rate-limiting step, with increasing ^{18}O -KIEs indicating a higher degree of O_2 reduction. For example, the ^{18}O -KIE of soybean lipoxygenase (1.009-1.012), reflects a rate-limiting electron transfer to O_2 to form an iron-superoxo species (Guy et al. 1992; Knapp and Klinman 2003). The ^{18}O -KIE of 1.015 ± 0.001 determined for hydroxyethyl phosphonate dioxygenase reflects a rate-limiting iron-hydroperoxo formation by hydrogen atom abstraction (Zhu et al. 2015). Finally, the ^{18}O -KIE of 1-aminocyclopropyl-1-carboxylic acid oxidase (1.0215 ± 0.005) reflects a rate-limiting iron-oxo formation (Mirica et al. 2008). For cytochrome-*c* oxidase, a rate-limiting hydrogen atom abstraction by an iron-bound superoxo species with



concomitant O-O bond cleavage and formation of a high-valent iron-oxo intermediate has been suggested (Yoshikawa and Shimada 2015). The corresponding ^{18}O -KIE of 1.0189 ± 0.0005 determined in this study is in agreement with both a hydrogen atom abstraction by a metal-superoxo species, as seen for many of the copper-dependent enzymes, as well as with the formation of a high-valent iron-oxo species as described for 1-aminocyclopropyl-1-carboxylic acid oxidase.

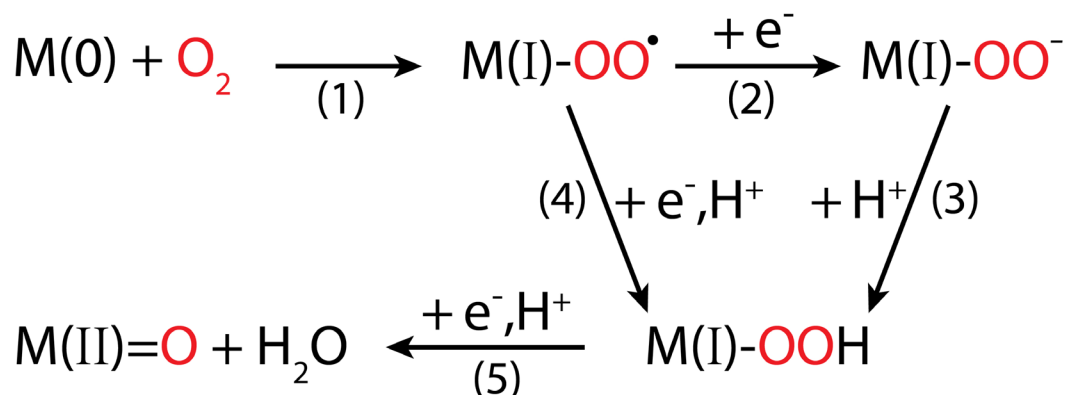


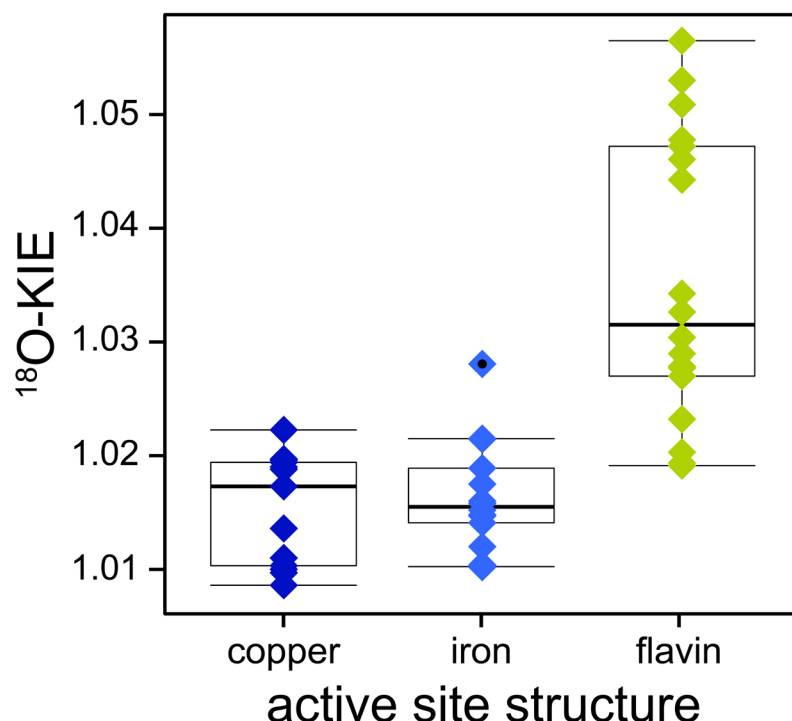
Figure 6. Simplified scheme of O_2 reduction steps performed by copper- and iron-dependent oxidases and oxygenases shown without interactions with (co-)substrates. M(0) indicates a metal ion in its most reduced state, which is typically Cu(I) or Fe(II), thus M(I) corresponds to either Cu(II) or Fe(III). M(II)=O only occurs in iron-dependent enzymes as a high-valent iron-oxo species (Fe(IV)=O).

5 Conclusions

The combined analysis of ^{18}O -KIEs of O_2 -consuming enzymes, determined in this and previous studies, enabled a comprehensive evaluation of the variability of kinetic isotope effects within and between different active site structures, as illustrated in Fig. 7. Notably, iron- and copper-dependent O_2 -consuming enzymes displayed a narrower range of ^{18}O -KIEs with lower magnitudes (1.009 - 1.028) compared to flavin-dependent enzymes (1.020 - 1.058). This variability likely reflects differences in electron transfer mechanisms, specifically inner- versus outer-sphere electron transfer. Within the flavin-dependent O_2 -consuming enzymes, the two distinct ranges of ^{18}O -KIEs likely correspond to two different O_2 reduction mechanisms, as discussed in section 4.1. Specifically, flavin-dependent enzymes with ^{18}O -KIEs below 1.035 are likely associated with a rate-limiting O_2^\bullet or FLOO^\bullet formation prior to FLOOH formation, potentially influenced by a rate-contributing O_2 binding step that masks the intrinsic ^{18}O -KIE. Conversely, flavin-dependent enzymes with ^{18}O -KIEs above 1.04 are suggested to follow the alternative O_2 reduction pathway, in which H_2O_2 and oxidized flavin are formed directly from FLH^\bullet and O_2^\bullet without the formation of FLOOH . Similarly, the copper-dependent O_2 -consuming enzymes investigated in this and previous studies can be assigned to one of two groups (see Fig. 5). Enzymes with ^{18}O -KIEs between 1.009 and 1.011 are likely characterized by a rate-limiting copper-superoxo formation. Enzymes with ^{18}O -KIEs between 1.017 and 1.022 are suggested to have a rate-limiting hydrogen atom abstraction leading to the formation of a copper-hydroperoxo species. Based on comparisons with calculated ^{18}O -EIEs, a rate-limiting copper-peroxo species formation for the second group remains



possible, however, existing experimental evidence favors a copper-hydroperoxo formation. The continuous increase in ^{18}O -KIEs observed for 13 iron-dependent O_2 -consuming enzymes, including cytochrome-*c* oxidase, reflects an increase in the extent of O_2 reduction during the rate-limiting step, aligning with increasing ^{18}O -EIEs calculated for metal-bound reactive oxygen intermediates. Consequently, if a ^{18}O -KIE is determined for an unknown O_2 -consuming enzymatic reaction, it appears that a value above 1.025 will typically be indicative of a flavin-dependent enzyme, whereas a value above 1.04 is characteristic for a flavin-dependent oxidase. By contrast, a ^{18}O -KIE below 1.015 can be confidently assigned to a metal-dependent enzyme. However, distinguishing between copper- and iron-dependent enzymes within this range is not possible. Overall, the patterns of isotopic fractionation of O_2 identified in this study can help clarify O_2 reduction mechanisms in other O_2 -consuming enzymes. Furthermore, the improved understanding of the variability in isotopic fractionation of O_2 at the enzyme level can assist in the interpretation of the variability in isotope fractionation of O_2 observed at the organism or ecosystem levels. For instance, the trends observed for copper-dependent O_2 -consuming enzymes may support the investigation of metabolic pathways carried out by environmentally relevant bacteria that possess copper-dependent O_2 -consuming enzymes, such as ammonia and methane monooxygenase. To further validate and support these findings, determining ^{18}O -KIEs of additional flavin-dependent monooxygenases, and copper-dependent O_2 -consuming enzymes in particular, would be highly valuable.



580 **Figure 7.** ^{18}O -KIEs of copper- (dark blue diamonds), iron- (light blue diamonds), and flavin-dependent (green diamonds) O_2 -consuming enzymes obtained in this and previous studies. A list of literature values including references can be found in Table S1 in the supplement. Boxes represent interquartile range and median values. The whiskers extend to observations that fall within 1.5 times above or below the box size; individual points with black dots represent observations that fall out of this range.

Appendix A: Experimental conditions by enzyme

585 All experiments were performed at room temperature ($23 \pm 1^\circ\text{C}$) with an initial O_2 concentration of $270 \pm 10 \mu\text{M}$, unless stated otherwise. Typically, 6-8 experiments were performed to determine the $K_m(\text{S})$ values with constant conditions, except for initial organic substrate concentrations. The $K_m(\text{O}_2)$ values were determined in single experiments at saturating substrate concentrations, unless noted otherwise. ^{18}O -KIEs were determined with duplicate or triplicate experiments at saturating substrate concentrations.

590 Alcohol oxidase

Experiments with $0.4\text{--}32 \text{ mg protein L}^{-1}$ alcohol oxidase were performed in a 50 mM phosphate buffer ($\text{pH } 7.5$). To calculate $K_m(\text{S})$ values, initial O_2 consumption rates were determined at 8 different initial methanol concentrations from 0.5 to 5 mM and at 8 different initial ethanol concentrations from 0.5 to 200 mM . Product inhibition was tested separately with 1 mM formaldehyde, 1 mM acetaldehyde, and 1 mM H_2O_2 . $K_m(\text{O}_2)$ values were determined with 10 mM methanol and 200 mM

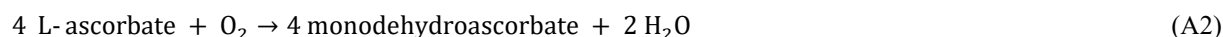


595 ethanol, respectively, at initial O₂ concentrations of 1200 ± 100 μM. Experiments with 2.5 mM methanol or 200 mM ethanol were performed to determine ¹⁸O-KIEs. Eq. A1 shows the reaction catalyzed by alcohol oxidase.



L-ascorbate oxidase

600 Experiments with 0.06-0.19 mg protein L⁻¹ L-ascorbate oxidase were performed in a 50 mM acetate buffer (pH 5.0). To calculate K_m(S), initial O₂ consumption rates were determined at 8 different initial L-ascorbic acid concentrations from 0.06 to 3 mM. Concentrations of L-ascorbic acid above 3 mM resulted in inhibition of enzymatic activity. Product inhibition was tested with a reaction solution after complete consumption of 0.27 mM L-ascorbic acid. The K_m(O₂) value and ¹⁸O-KIE were determined with 2.5 mM and 2 mM L-ascorbic acid, respectively. Eq. A2 shows the reaction catalyzed by L-ascorbate oxidase.



Bilirubin oxidase

605 Experiments with 0.7-2.5 mg protein L⁻¹ bilirubin oxidase were performed in a 100 mM Tris-HCl buffer (pH 8.5). To calculate K_m(S), initial O₂ consumption rates were determined at 8 different initial bilirubin concentrations from 0.025 to 1 mM. Product inhibition was tested with a reaction solution after complete consumption of 0.3 mM bilirubin. The K_m(O₂) value and ¹⁸O-KIE were determined with 1 mM bilirubin. Eq. A3 shows the reaction catalyzed by bilirubin oxidase.



Cholesterol oxidase

615 Experiments with 1.3-11 mg protein L⁻¹ cholesterol oxidase were performed in a 50 mM phosphate buffer (pH 7.5) with 1% (v/v) Thesit® and 10 % (v/v) isopropanol. To calculate K_m(S), initial O₂ consumption rates were determined at 6 different initial cholesterol concentrations from 0.1 to 1 mM. Product inhibition was tested separately with 0.3 and 1 mM H₂O₂ and with a reaction solution after complete consumption of 0.3 mM cholesterol. The K_m(O₂) value and ¹⁸O-KIE were determined with 1.5 mM cholesterol. Eq. A4 shows the reaction catalyzed by cholesterol oxidase.

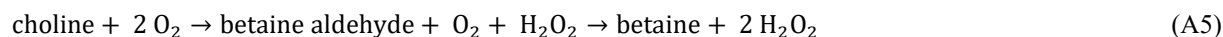


Choline oxidase

620 Experiments with 3-10 mg/L choline oxidase were performed in a 50 mM phosphate buffer (pH 7.5). To calculate K_m(S), initial O₂ consumption rates were determined at 8 different initial choline concentrations from 0.075 to 4.5 mM. Product

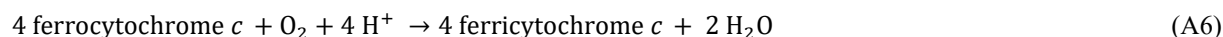


inhibition was tested separately with 0.3 mM H₂O₂ and 0.3 mM betaine. The K_m(O₂) value and ¹⁸O-KIE were determined with 10 mM and 2.5 mM choline, respectively. Eq. A5 shows the reaction catalyzed by choline oxidase.



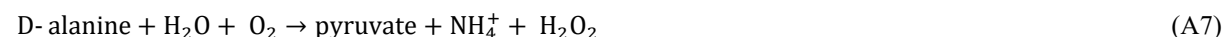
Cytochrome-*c* oxidase

625 Experiments with 1.5-2.3 mg protein L⁻¹ cytochrome-*c* oxidase were performed in a 10 mM phosphate buffer (pH 7.5) with 50 mM NaCl. K_m(S) was not determined. Product inhibition was not tested. Experiments to determine K_m(O₂) and ¹⁸O-KIE were performed with 25 μM cytochrome *c* and 3 mM ascorbic acid. Ascorbic acid was used to recycle the substrate by abiotically reducing ferricytochrome *c* to ferrocycytochrome *c*. Eq. A6 shows the reaction catalyzed by cytochrome-*c* oxidase.



630 D-amino-acid oxidase

Experiments with 1.8-5.9 mg protein L⁻¹ D-amino-acid oxidase were performed in a 50 mM Tris-HCl buffer (pH 8.2). To calculate K_m(S), initial O₂ consumption rates were determined at 8 different initial D-alanine concentrations from 0.3 to 20 mM. Product inhibition was tested separately with 0.3 mM H₂O₂ as well as with 0.27 mM ammonium and 0.27 mM pyruvate. The K_m(O₂) value and ¹⁸O-KIE were determined with 20 mM D-alanine. Eq. A7 shows the reaction catalyzed by D-amino-
635 acid oxidase.



Diamine oxidase

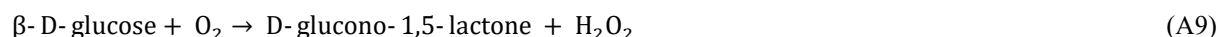
Experiments with 800-5000 mg/L diamine oxidase were performed in a 50 mM phosphate buffer (pH 7.2). To calculate K_m(S), initial O₂ consumption rates were determined at 6 different initial histamine concentrations from 0.025 to 0.5 mM. Concentrations of histamine above 0.5 mM resulted in inhibition of enzymatic activity. Product inhibition was tested with a reaction solution after complete consumption of 0.25 mM histamine. The K_m(O₂) value and ¹⁸O-KIE were determined with 0.4 mM histamine. Eq. A8 shows the reaction catalyzed by diamine oxidase. The enzyme provided by the manufacturer was tested positively for catalase activity. Thus, the H₂O₂ formed during the reaction of histamine with diamine oxidase was immediately converted to O₂ and H₂O (see section 3.3 for implications of O₂ formation on ¹⁸O-KIE determination).





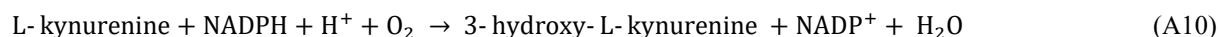
Glucose oxidase

Experiments with 9-41 mg protein L⁻¹ glucose oxidase were performed in a 100 mM acetate buffer (pH 5.0). To calculate K_m(S) values, initial O₂ consumption rates were determined at 7 different initial D-glucose concentrations from 0.45 to 70 mM and at 11 different initial D-mannose concentrations from 0.45 to 100 mM. Product inhibition was tested separately with 0.3 mM H₂O₂ and with reaction solutions after complete consumption of 0.45 mM D-mannose and 0.27 mM D-glucose, respectively. The K_m(O₂) values were determined with 40 mM D-glucose and 100 mM D-mannose, respectively. The ¹⁸O-KIEs were determined with 40 mM D-glucose or 40 mM D-mannose. Eq. A9 shows the reaction catalyzed by glucose oxidase with D-glucose.



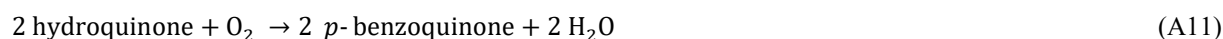
Kynurenine 3-monooxygenase

Experiments with 3-9 mg/L kynurenine 3-monooxygenase (KMO) were performed in a 20 mM HEPES buffer (pH 7.5). K_m(S) was not determined. Product inhibition was tested with a reaction solution after complete consumption of 0.3 mM L-kynurenine. To calculate K_m(O₂), initial O₂ consumption rates were determined with 1 mM L-kynurenine, 0.5 mM NADPH and 2 mM dithiothreitol at 8 different initial O₂ concentrations from 25 to 260 μM. The ¹⁸O-KIE was determined with 1 mM L-kynurenine, 0.5 mM NADPH and 2 mM dithiothreitol. Eq. A10 shows the reaction catalyzed by KMO.



Laccase from *Agaricus bisporus*

Experiments with 10-100 mg/L laccase from *Agaricus bisporus* were performed in a 50 mM acetate buffer (pH 5.5). To calculate K_m(S), initial O₂ consumption rates were determined at 10 different initial hydroquinone concentrations from 0.05 to 20 mM. Product inhibition was tested with 0.54 mM *p*-benzoquinone. The K_m(O₂) value and ¹⁸O-KIE were determined with 15 mM hydroquinone. Eq. A11 shows the reaction catalyzed by laccase with hydroquinone.



Laccase from *Trametes versicolor*

Experiments with 10-100 mg/L laccase from *Trametes versicolor* were performed in a 50 mM acetate buffer (pH 5.5). To calculate K_m(S) values, initial O₂ consumption rates were determined at 10 different initial hydroquinone concentrations from 0.005 to 15 mM and at 7 different initial ABTS concentrations from 0.06 to 7.5 mM. Product inhibition was tested with 0.54 mM *p*-benzoquinone and with a reaction solution after complete consumption of 1.2 mM ABTS. The K_m(O₂) values were determined from a single experiment with 15 mM hydroquinone and from initial O₂ consumption rates with 3.8 mM ABTS



and 6 different initial O₂ concentrations from 25 to 265 μM. The ¹⁸O-KIEs were determined with 7.5 mM hydroquinone and
675 4 mM ABTS, respectively. Eq. A12 shows the reaction catalyzed by laccase with ABTS.



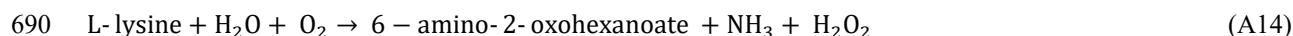
L-lactate oxidase

To calculate K_m(S), initial O₂ consumption rates were determined at six different initial L-lactic acid concentrations from 0.1
680 to 10 mM in a 50 mM phosphate buffer (pH 7.0) with 20 mM KCl and 2.3 mg/L enzyme. Product inhibition was tested
separately with 0.3 mM pyruvate and 0.3 mM H₂O₂. The K_m(O₂) value and ¹⁸O-KIE were determined in a 50 mM HEPES
buffer (pH 7.0) with 50 mM KCl containing either 10 mM L-lactic acid and 2.3 mg/L enzyme or 5 mM L-lactic acid and 1.2
mg/L enzyme. Eq. A13 shows the reaction catalyzed by L-lactate oxidase.



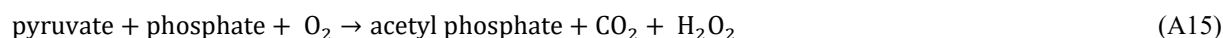
L-lysine oxidase

685 Experiments with 0.3-2.2 mg protein L⁻¹ L-lysine oxidase were performed in a 50 mM phosphate buffer (pH 8.0). To calculate
K_m(S), initial O₂ consumption rates were determined at 6 different initial L-lysine concentrations from 0.01 to 2 mM. Product
inhibition was tested separately with 0.3 mM H₂O₂ and with a reaction solution after complete consumption of 0.3 mM L-
lysine. The K_m(O₂) value and ¹⁸O-KIE were determined with 2.3 mM and 2 mM L-lysine, respectively. Eq. A14 shows the
reaction catalyzed by L-lysine oxidase.



Pyruvate oxidase

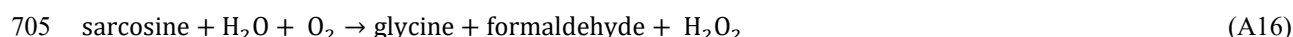
Experiments with 0.3-1.3 mg protein L⁻¹ pyruvate oxidase were performed in a 50 mM phosphate buffer (pH 6.7) with 1 mM
thiamine diphosphate, 1 mM MnSO₄ and 10 μM FAD. K_m(S) was not determined. Product inhibition was tested separately
with 0.27 mM sodium bicarbonate and 0.27 mM H₂O₂. The K_m(O₂) value was determined with 100 mM pyruvate. The ¹⁸O-
695 KIE was determined with 25, 50, and 100 mM pyruvate. Prior to starting an experiment, pyruvate oxidase was incubated with
1 mM thiamine diphosphate, 1 mM MnSO₄, 10 μM FAD, and 5-100 mM pyruvate for 10 minutes at room temperature. Eq.
A15 shows the reaction catalyzed by pyruvate oxidase.





Sarcosine oxidase

700 Experiments with 0.5-10 mg/L sarcosine oxidase were performed in a 100 mM Tris-HCl buffer (pH 8.3). To calculate $K_m(S)$ values, initial O_2 consumption rates were determined at 6 different initial sarcosine concentrations from 5 to 100 mM. Product inhibition was tested separately with 0.3 mM glycine, 1 mM formaldehyde, and 0.3 mM H_2O_2 . The $K_m(O_2)$ value and ^{18}O -KIE were determined with 100 mM and 50 mM sarcosine, respectively. Eq. A16 shows the reaction catalyzed by sarcosine oxidase.



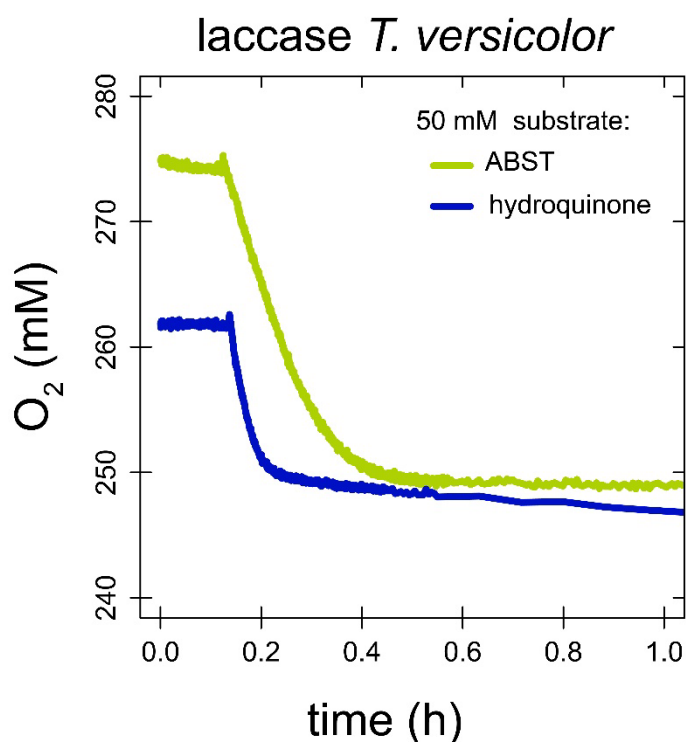
Appendix B: Enzyme assays for ^{18}O -kinetic isotope effects in O_2 -purged buffer

Alcohol, choline, and L-lysine oxidase exhibited $K_m(O_2)$ values above air-saturation. For this reason, in addition to the enzyme assays described in section 2.2, the ^{18}O -kinetic isotope effects (^{18}O -KIEs) of these enzymes were additionally performed in O_2 -purged buffer solutions under otherwise identical experimental conditions (see Appendix A). Enzyme assays with alcohol and choline oxidase were performed each in 12 identically filled crimp-top vials as described in section 2.2. Enzyme assays with L-lysine oxidase were performed directly in 8 Exetainers that were sacrificed at different time-points. Exetainers were filled completely with assay solution and closed, before a small volume of enzyme or substrate solution was injected through the septa to initiate the reaction. Prior to sampling, the remaining O_2 concentration was measured with a fiber-optic oxygen microsensor. After measuring O_2 concentrations, the reaction was stopped by injecting 200 μL of a 3 M HCl solution through the septa with a gas-tight glass syringe, while simultaneously piercing the septa with a small exhaust needle. After enzyme injection, before measuring O_2 concentrations, and after HCl additions, Exetainers were shaken vigorously. To create a He headspace in the Exetainer, 5 mL assay solution was removed with a 10 mL gas-tight glass while the Exetainer was connected to a slow stream of He gas. Procedural blanks were prepared by completely filling Exetainers with N_2 -purged water in an anaerobic glove box with a N_2 atmosphere (GS GLOVEBOX Systemtechnik, residual O_2 content < 1 ppm). Under ambient atmosphere, 200 μL NaOH were then injected through the septa into the closed Exetainer. Control samples and quantification standards were prepared by completely filling Exetainers with leftover assay solution without enzyme or with air-equilibrated water, respectively. For blanks, control samples, and quantification standards, a 5 mL He headspace was created as described for the assay samples. The resulting ^{18}O -KIEs were 1.029 ± 0.004 for alcohol oxidase, 1.019 ± 0.002 for choline oxidase, and 1.04 ± 0.01 for L-lysine oxidase.



725 Appendix C: Substrate-to-O₂ consumption stoichiometries of laccase

With laccase from *T. versicolor*, the substrate-to-O₂ consumption stoichiometry was determined for the two substrates hydroquinone and ABTS. Enzyme assays were performed in air-saturated buffer as described in section 2.1, but with a limiting amount of substrate. O₂ concentrations were stable before substrate addition. After the addition of 50 μM hydroquinone, O₂ concentrations decreased rapidly from 275 μM to 249 μM and remained stable thereafter. Assuming all hydroquinone was consumed, this decrease in O₂ concentration corresponds to a substrate-to-O₂ consumption stoichiometry of 1.92 to 1. After the addition of 51 μM ABTS, O₂ concentrations decreased rapidly from 262 μM to 249 μM and slowly thereafter. It is likely that the initial fast decrease in O₂ concentration is the result of the enzymatic reaction catalyzed by laccase, while the later slower O₂ consumption is a result of abiotic reaction between the radical product ABTS[•] and O₂. Assuming all ABTS was consumed in the initial fast reaction, the substrate-to-O₂ consumption stoichiometry was 4.0 to 1.



735

Figure C1. O₂ consumption profiles by laccase from *T. versicolor* when supplied with 50 μM ABTS (green line) or hydroquinone (blue line).

Data availability

All data presented in this study are available at <https://doi.org/10.5281/zenodo.14765061>.



740 Author contribution

CFMC contributed to conceptualization, investigation, methodology, visualization, writing (original draft, review and editing). MFL contributed to supervision, writing (review and editing). SGP contributed to conceptualization, funding acquisition, methodology, supervision, writing (review and editing).

Competing interests

745 The authors declare that they have no conflict of interest.

Acknowledgments

We thank Thomas Kuhn for his support with IRMS measurements.

Financial support

This work was supported by the Swiss National Science Foundation (Grant no. PZ00P2_186083).

750 References

- Ash, J.L., Hu, H., Yeung, L.Y.: What fractionates oxygen isotopes during respiration? Insights from multiple isotopologue measurements and theory, *ACS Earth and Space Chemistry*, 4, 50–66, <https://doi.org/10.1021/acsearthspacechem.9b00230>, 2020.
- Bauer, J.A., Zámocká, M., Majtán, J., Bauerová-Hlinková, V.: Glucose oxidase, an enzyme “Ferrari”: Its structure, function, 755 production and properties in the light of various industrial and biotechnological applications, *Biomolecules*, 12, 472, <https://doi.org/10.3390/biom12030472>, 2022.
- Bender, M., Sowers, T., Dickson, M.L., Orchardo, J., Grootes, P., Mayewski, P.A., Meese, D.A.: Climate correlations between Greenland and Antarctica during the past 100,000 years, *Nature*, 372, 663–666, <https://doi.org/10.1038/372663a0>, 1994.
- Bender, M.L.: The $\delta^{18}\text{O}$ of dissolved O_2 in seawater: A unique tracer of circulation and respiration in the deep sea, *J. Geophys. 760 Res.*, 95, 22243–22252. <https://doi.org/10.1029/JC095iC12p22243>, 1990.
- Bento, I., Carrondo, M.A., Lindley, P.F.: Reduction of dioxygen by enzymes containing copper, *J. Biol. Inorg. Chem.*, 11, 539–547, <https://doi.org/10.1007/s00775-006-0114-9>, 2006.
- Bernhardt, R.: Cytochromes P450 as versatile biocatalysts, *J. Biotechnol.*, 124, 128–145, <https://doi.org/10.1016/j.jbiotec.2006.01.026>, 2006.



- Blank, L.M., Ebert, B.E., Buehler, K., Bühler, B.: Redox biocatalysis and metabolism: Molecular mechanisms and metabolic network analysis, *Antioxid. Redox Sign.*, 13, 349–394, <https://doi.org/10.1089/ars.2009.2931>, 2010.
- Blunier, T., Bender, M.L., Barnett, B., von Fischer, J.C.: Planetary fertility during the past 400 ka based on the triple isotope composition of O₂ in trapped gases from the Vostok ice core, *Clim. Past*, 8, 1509–1526, <https://doi.org/10.5194/cp-8-1509-2012>, 2012.
- Bocaniov, S.A., Schiff, S.L., Smith, R.E.H.: Non steady-state dynamics of stable oxygen isotopes for estimates of metabolic balance in large lakes, *J. Great Lakes Res.*, 41, 719–729, <https://doi.org/10.1016/j.jglr.2015.05.013>, 2015.
- Bocaniov, S.A., Schiff, S.L., Smith, R.E.H.: Plankton metabolism and physical forcing in a productive embayment of a large oligotrophic lake: Insights from stable oxygen isotopes, *Freshwater Biol.*, 57, 481–496, <https://doi.org/10.1111/j.1365-2427.2011.02715.x>, 2012.
- Bogard, M.J., Vachon, D., St.-Gelais, N.F., del Giorgio, P.A.: Using oxygen stable isotopes to quantify ecosystem metabolism in northern lakes, *Biogeochemistry*, 133, 347–364, <https://doi.org/10.1007/s10533-017-0338-5>, 2017.
- Bugg, T.D.H.: Oxygenases: Mechanisms and structural motifs for O₂ activation, *Curr. Opin. Chem. Biol.*, 5, 550–555, [https://doi.org/10.1016/S1367-5931\(00\)00236-2](https://doi.org/10.1016/S1367-5931(00)00236-2), 2001.
- Chaiyen, P., Fraaije, M.W., Mattevi, A.: The enigmatic reaction of flavins with oxygen, *Trends Biochem. Sci.*, 37, 373–380, <https://doi.org/10.1016/j.tibs.2012.06.005>, 2012.
- Cheah, M.H., Millar, A.H., Myers, R.C., Day, D.A., Roth, J., Hillier, W., Badger, M.R.: Online oxygen kinetic isotope effects using membrane inlet mass spectrometry can differentiate between oxidases for mechanistic studies and calculation of their contributions to oxygen consumption in whole tissues, *Anal. Chem.*, 86, 5171–5178, <https://doi.org/10.1021/ac501086n>, 2014.
- Coplen, T.B.: Guidelines and recommended terms for expression of stable-isotope-ratio and gas-ratio measurement results, *Rapid Commun. Mass Sp.*, 25, 2538–2560, <https://doi.org/10.1002/rcm.5129>, 2011.
- Costas, M., Mehn, M.P., Jensen, M.P., Que, L.: Dioxygen activation at mononuclear nonheme iron active sites: Enzymes, models, and intermediates, *Chem. Rev.*, 104, 939–986, <https://doi.org/10.1021/cr020628n>, 2004.
- Crozier, K.R., Moran, G.R.: Heterologous expression and purification of kynurenine-3-monooxygenase from *Pseudomonas fluorescens* strain 17400, *Protein Expres. Purif.*, 51, 324–333, <https://doi.org/10.1016/j.pep.2006.07.024>, 2007.
- de Carvalho, C.F.M., Lehmann, M.F., Pati, S.G.: Improving the accuracy of $\delta^{18}\text{O}$ and $\delta^{17}\text{O}$ values of O₂ measured by continuous-flow isotope-ratio mass spectrometry with a multipoint isotope-ratio calibration, *Rapid Commun. Mass Sp.*, 38, <https://doi.org/10.1002/rcm.9652>, 2024.
- Epstein, S., Zeiri, L.: Oxygen and carbon isotopic compositions of gases respired by humans, *P. Natl. Acad. Sci. USA*, 85, 1727–1731, <https://doi.org/10.1073/pnas.85.6.1727>, 1988.
- Evans, J.P., Ahn, K., Klinman, J.P.: Evidence that dioxygen and substrate activation are tightly coupled in dopamine β -monooxygenase: Implications for the reactive oxygen species, *J. Biol. Chem.*, 278, 49691–49698, <https://doi.org/10.1074/jbc.M300797200>, 2003.



- Feldman, D.E., Yost, H.T., Benson, B.B.: Oxygen isotope fractionation in reactions catalyzed by enzymes, *Science*, 129, 146–
800 147, <https://doi.org/10.1126/science.129.3342.146>, 1959.
- Finney, J., Moon, H.J., Ronnebaum, T., Lantz, M., Mure, M.: Human copper-dependent amine oxidases, *Arch. Biochem. Biophys.*, 546, 19–32, <https://doi.org/10.1016/j.abb.2013.12.022>, 2014.
- Francisco, W.A., Blackburn, N.J., Klinman, J.P.: Oxygen and hydrogen isotope effects in an active site tyrosine to phenylalanine mutant of peptidylglycine α -hydroxylating monooxygenase: Mechanistic implications, *Biochemistry-US*,
805 42, 1813–1819, <https://doi.org/10.1021/bi020592t>, 2003.
- Frey, P.A., Hegeman, A.D. (Eds.): *Enzymatic Reaction Mechanisms*, Oxford University Press, Oxford, United Kingdom, 710 pp., <https://doi.org/10.1093/oso/9780195122589.003.0021>, 2007.
- Gammons, C.H., Henne, W., Poulson, S.R., Parker, S.R., Johnston, T.B., Dore, J.E., Boyd, E.S.: Stable isotopes track biogeochemical processes under seasonal ice cover in a shallow, productive lake, *Biogeochemistry*, 120, 359–379,
810 <https://doi.org/10.1007/s10533-014-0005-z>, 2014.
- Guengerich, F.P.: Mechanisms of cytochrome P450 substrate oxidation: MiniReview, *J. Biochem. Mol. Toxic.*, 21, 163–168, <https://doi.org/10.1002/jbt.20174>, 2007.
- Guy, R.D., Berry, J.A., Fogel, M.L., Turpin, D.H., Weger, H.G.: Fractionation of the stable isotopes of oxygen during respiration by plants – The basis for a new technique, in: *Molecular, Biochemical and Physiological Aspects of Plant Respiration*, edited by: Lambers, H., van der Plas, L.H.W., SPB Academic Publishing bv, The Hague, Netherlands, 443–
815 453, 1992.
- Guy, R.D., Berry, J.A., Fogel, M.L., Hoering, T.C.: Differential fractionation of oxygen isotopes by cyanide-resistant and cyanide-sensitive respiration in plants, *Planta*, 177, 483–491, <https://doi.org/10.1007/BF00392616>, 1989.
- Guy, R.D., Fogel, M.L., Berry, J.A.: Photosynthetic fractionation of the stable isotopes of oxygen and carbon, *Plant Physiol.*,
820 101, 37–47, <https://doi.org/10.1104/pp.101.1.37>, 1993.
- Guy, R.D., Fogel, M.L., Berry, J.A., Hoering, T.C.: Isotope fractionation during oxygen production and consumption by plants, in: *Progress in Photosynthesis Research*, edited by: Biggins, J., Springer Netherlands, Dordrecht, Netherlands, 597–600, https://doi.org/10.1007/978-94-017-0516-5_127, 1987.
- Hayles, J.A., Killingsworth, B.A.: Constraints on triple oxygen isotope kinetics, *Chem. Geol.*, 589,
825 <https://doi.org/10.1016/j.chemgeo.2021.120646>, 2022.
- Helman, Y., Barkan, E., Eisenstadt, D., Luz, B., Kaplan, A.: Fractionation of the three stable oxygen isotopes by oxygen-producing and oxygen-consuming reactions in photosynthetic organisms, *Plant Physiol.*, 138, 2292–2298, <https://doi.org/10.1104/pp.105.063768>, 2005.
- Hendricks, M.B., Bender, M.L., Barnett, B.A.: Net and gross O₂ production in the Southern Ocean from measurements of
830 biological O₂ saturation and its triple isotope composition, *Deep Sea Research Part I: Oceanographic Research Papers*, 51, 1541–1561, <https://doi.org/10.1016/j.dsr.2004.06.006>, 2004.



- Hendricks, M.B., Bender, M.L., Barnett, B.A., Strutton, P., Chavez, F.P.: Triple oxygen isotope composition of dissolved O₂ in the equatorial Pacific: A tracer of mixing, production, and respiration, *J. Geophys. Res.-Oceans*, 110, 1–17, <https://doi.org/10.1029/2004JC002735>, 2005.
- 835 Hotchkiss, E.R., Hall, R.O.: High rates of daytime respiration in three streams: Use of $\delta^{18}\text{O}$ -O₂ and O₂ to model diel ecosystem metabolism, *Limnol. Oceanogr.*, 59, 798–810, <https://doi.org/10.4319/lo.2014.59.3.0798>, 2014.
- Huang, X., Groves, J.T.: Oxygen activation and radical transformations in heme proteins and metalloporphyrins, *Chem. Rev.*, 118, 2491–2553, <https://doi.org/10.1021/acs.chemrev.7b00373>, 2018.
- Humphreys, K.J., Mirica, L.M., Wang, Y., Klinman, J.P.: Galactose oxidase as a model for reactivity at a copper superoxide
840 center, *J. Am. Chem. Soc.*, 131, 4657–4663, <https://doi.org/10.1021/ja807963e>, 2009.
- Juranek, L.W., Quay, P.D.: Using triple isotopes of dissolved oxygen to evaluate global marine productivity, *Annu. Rev. Mar. Sci.*, 5, 503–524, <https://doi.org/10.1146/annurev-marine-121211-172430>, 2013.
- Jurikova, H., Guha, T., Abe, O., Shiah, F.K., Wang, C.H., Liang, M.C.: Variations in triple isotope composition of dissolved oxygen and primary production in a subtropical reservoir, *Biogeosciences*, 13, 6683–6698, [https://doi.org/10.5194/bg-](https://doi.org/10.5194/bg-13-6683-2016)
845 13-6683-2016, 2016.
- Kiddon, J., Bender, M.L., Orchardo, J., Caron, D.A., Goldman, J.C., Dennett, M.: Isotopic fractionation of oxygen by respiring marine organisms, *Global Biogeochem. Cy.*, 7, 679–694, <https://doi.org/10.1029/93GB01444>, 1993.
- Kiss, D.J., Ferenczy, G.G.: A detailed mechanism of the oxidative half-reaction of D-amino acid oxidase: Another route for flavin oxidation, *Org. Biomol. Chem.*, 17, 7973–7984, <https://doi.org/10.1039/C9OB00975B>, 2019.
- 850 Klinman, J.P.: How do enzymes activate oxygen without inactivating themselves?, *Accounts Chem. Res.*, 40, 325–333, <https://doi.org/10.1021/ar6000507>, 2007.
- Knapp, M.J., Klinman, J.P.: Kinetic studies of oxygen reactivity in soybean lipoxygenase-1, *Biochemistry-US*, 42, 11466–11475, <https://doi.org/10.1021/bi0300884>, 2003.
- Kroopnick, P., Craig, H.: Oxygen isotope fractionation in dissolved oxygen in the deep sea, *Earth Planet. Sc. Lett.*, 32, 375–
855 389, [https://doi.org/10.1016/0012-821X\(76\)90078-9](https://doi.org/10.1016/0012-821X(76)90078-9), 1976.
- Lanci, M.P., Smirnov, V.V., Cramer, C.J., Gauchenova, E.V., Sundermeyer, J., Roth, J.P.: Isotopic probing of molecular oxygen activation at copper(I) sites, *J. Am. Chem. Soc.*, 129, 14697–14709, <https://doi.org/10.1021/ja074620c>, 2007.
- Laskar, A.H., Peethambaran, R., Adnew, G.A., Röckmann, T.: Measurement of $^{18}\text{O}^{18}\text{O}$ and $^{17}\text{O}^{18}\text{O}$ in atmospheric O₂ using the 253 Ultra mass spectrometer and applications to stratospheric and tropospheric air samples, *Rapid Commun. Mass Sp.*, 33, 981–994, <https://doi.org/10.1002/rcm.8434>, 2019.
- 860 Levine, N.M., Bender, M.L., Doney, S.C.: The $\delta^{18}\text{O}$ of dissolved O₂ as a tracer of mixing and respiration in the mesopelagic ocean, *Global Biogeochem. Cy.*, 23, 1–12, <https://doi.org/10.1029/2007GB003162>, 2009.
- Liu, J., Chakraborty, S., Hosseinzadeh, P., Yu, Y., Tian, S., Petrik, I., Bhagi, A., Lu, Y.: Metalloproteins containing cytochrome, iron-sulfur, or copper redox centers, *Chem. Rev.*, 114, 4366–4369, <https://doi.org/10.1021/cr400479b>,
865 2014.



- Luz, B., Barkan, E.: Assessment of oceanic productivity with the triple-isotope composition of dissolved oxygen, *Science*, 288, 2028–2031, <https://doi.org/10.1126/science.288.5473.2028>, 2000.
- Luz, B., Barkan, E.: The isotopic ratios of $^{17}\text{O}/^{16}\text{O}$ and $^{18}\text{O}/^{16}\text{O}$ in molecular oxygen and their significance in biogeochemistry, *Geochim. Cosmochim. Ac.*, 69, 1099–1110, <https://doi.org/10.1016/j.gca.2004.09.001>, 2005.
- 870 Luz, B., Barkan, E.: Net and gross oxygen production from O_2/Ar , $^{17}\text{O}/^{16}\text{O}$ and $^{18}\text{O}/^{16}\text{O}$ ratios, *Aquat. Microb. Ecol.*, 56, 133–145, <https://doi.org/10.3354/ame01296>, 2009.
- Luz, B., Barkan, E.: Oxygen isotope fractionation in the ocean surface and $^{18}\text{O}/^{16}\text{O}$ of atmospheric O_2 , *Global Biogeochem. Cy.*, 25, 17–18, <https://doi.org/10.1029/2011GB004178>, 2011.
- Luz, B., Barkan, E., Sagi, Y., Yacobi, Y.Z.: Evaluation of community respiratory mechanisms with oxygen isotopes: A case
875 study in Lake Kinneret, *Limnol. Oceanogr.*, 47, 33–42, <https://doi.org/10.4319/lo.2002.47.1.0033>, 2002.
- Macheroux, P., Massey, V., Thiele, D.J., Volokita, M.: Expression of spinach glycolate oxidase in *Saccharomyces cerevisiae*: purification and characterization, *Biochemistry-US*, 30, 4612–4619, <https://doi.org/10.1021/bi00232a036>, 1991.
- Mader, M., Schmidt, C., van Geldern, R., Barth, J.A.C.: Dissolved oxygen in water and its stable isotope effects: A review, *Chem. Geol.*, 473, 10–21, <https://doi.org/10.1016/j.chemgeo.2017.10.003>, 2017.
- 880 Malmstrom, B.G.: Enzymology of Oxygen, *Annu. Rev. Biochem.*, 51, 21–59, <https://doi.org/10.1146/annurev.bi.51.070182.000321>, 1982.
- Massey, V.: The reactivity of oxygen with flavoproteins, *Int. Congr. Ser.*, 1233, 3–11, [https://doi.org/10.1016/S0531-5131\(02\)00519-8](https://doi.org/10.1016/S0531-5131(02)00519-8), 2002.
- Mattevi, A.: To be or not to be an oxidase: challenging the oxygen reactivity of flavoenzymes, *Trends Biochem. Sci.*, 31, 276–
885 283, <https://doi.org/10.1016/j.tibs.2006.03.003>, 2006.
- McDonald, A.G., Boyce, S., Tipton, K.F.: ExplorEnz: The primary source of the IUBMB enzyme list, *Nucleic Acids Res.*, 37, D593–D597, <https://doi.org/10.1093/nar/gkn582>, 2009.
- Medda, R., Padiglia, A., Floris, G.: Plant copper-amine oxidases, *Phytochemistry*, 39, 1–9, [https://doi.org/10.1016/0031-9422\(94\)00756-J](https://doi.org/10.1016/0031-9422(94)00756-J), 1995.
- 890 Merle, P., Kadenbach, B.: Kinetic and structural differences between cytochrome c oxidases from beef liver and heart, *Eur. J. Biochem.*, 125, 239–244, <https://doi.org/10.1111/j.1432-1033.1982.tb06674.x>, 1982.
- Miller, M.F.: Isotopic fractionation and the quantification of ^{17}O anomalies in the oxygen three-isotope system: an appraisal and geochemical significance, *Geochim. Cosmochim. Ac.*, 66, 1881–1889, [https://doi.org/10.1016/S0016-7037\(02\)00832-3](https://doi.org/10.1016/S0016-7037(02)00832-3), 2002.
- 895 Mills, S.A., Goto, Y., Su, Q., Plastino, J., Klinman, J.P.: Mechanistic comparison of the cobalt-substituted and wild-type copper amine oxidase from *Hansenula polymorpha*, *Biochemistry-US*, 41, 10577–10584, <https://doi.org/10.1021/bi0200864>, 2002.
- Mirica, L.M., McCusker, K.P., Munos, J.W., Liu, H., Klinman, J.P.: ^{18}O kinetic isotope effects in non-heme iron enzymes: Probing the nature of Fe/O_2 intermediates, *J. Am. Chem. Soc.*, 130, 8122–8123, <https://doi.org/10.1021/ja800265s>, 2008.



- 900 Mukherjee, A., Smirnov, V.V., Lanci, M.P., Brown, D.E., Shepard, E.M., Dooley, D.M., Roth, J.P.: Inner-sphere mechanism for molecular oxygen reduction catalyzed by copper amine oxidases, *J. Am. Chem. Soc.*, 130, 9459–9473, <https://doi.org/10.1021/ja801378f>, 2008.
- Mure, M., Mills, S.A., Klinman, J.P.: Catalytic mechanism of the topa quinone containing copper amine oxidases, *Biochemistry-US*, 41, 9269–9278, <https://doi.org/10.1021/bi020246b>, 2002.
- 905 Northrop, D.B.: On the meaning of K_m and V/K in enzyme kinetics, *J. Chem. Educ.*, 75, 1153, <https://doi.org/10.1021/ed075p1153>, 1998.
- Osborne, R.L., Klinman, J.P.: Insights into the proposed copper–oxygen Intermediates that regulate the mechanism of reactions catalyzed by dopamine β -monooxygenase, peptidylglycine α -hydroxylating monooxygenase, and tyramine β -monooxygenase, in: *Copper-Oxygen Chemistry*, edited by: Karlin, K.D., Itoh, S., John Wiley & Sons Inc., Hoboken, United States, 1–22, <https://doi.org/10.1002/9781118094365.ch1>, 2011.
- 910 Özkılıç, Y., Tüzün, N.Ş.: Mechanism of Kynurenine 3-Monooxygenase-Catalyzed Hydroxylation Reaction: A Quantum Cluster Approach, *J. Phys. Chem. A*, 123, 3149–3159, <https://doi.org/10.1021/acs.jpca.8b11831>, 2019.
- Pati, S.G., Bolotin, J., Brennwald, M.S., Kohler, H.P.E., Werner, R.A., Hofstetter, T.B.: Measurement of oxygen isotope ratios ($^{18}\text{O}/^{16}\text{O}$) of aqueous O_2 in small samples by gas chromatography/isotope ratio mass spectrometry, *Rapid Commun. Mass Sp.*, 30, 684–690, <https://doi.org/10.1002/rcm.7481>, 2016.
- 915 Pati, S.G., Bopp, C.E., Kohler, H.P.E., Hofstetter, T.B.: Substrate-specific coupling of O_2 activation to hydroxylations of aromatic compounds by Rieske non-heme iron dioxxygenases, *ACS Catal.*, 12, 6444–6456, <https://doi.org/10.1021/acscatal.2c00383>, 2022.
- Petit, J.R., Jouzel, J., Raynaud, D., Barkov, N.I., Barnola, J.M., Basile, I., Bender, M., Chappellaz, J., Davis, M., Delaygue, G., Delmotte, M., Kotlyakov, V.M., Legrand, M., Lipenkov, V.Y., Lorius, C., Pépin, L., Ritz, C., Saltzman, E., Stievenard, M.: Climate and atmospheric history of the past 420,000 years from the Vostok ice core, Antarctica, *Nature*, 399, 429–436, <https://doi.org/10.1038/20859>, 1999.
- Pimviriyakul, P., Chaiyen, P.: Overview of flavin-dependent enzymes, in: *The Enzymes – Flavin-Dependent Enzymes: Mechanisms, Structures and Applications*, edited by: Chaiyen, P., Tamanoi, F., Academic Press, Cambridge, United States, 1–36, <https://doi.org/10.1016/bs.enz.2020.06.006>, 2020.
- 925 R Core Team: R: A language and environment for statistical computing, 2023.
- Rafelski, L.E., Paplawsky, B., Keeling, R.F.: Continuous measurements of dissolved O_2 and oxygen isotopes in the Southern California coastal ocean, *Mar. Chem.*, 174, 94–102, <https://doi.org/10.1016/j.marchem.2015.05.011>, 2015.
- Ribas-Carbo, M., Berry, J.A., Yakir, D., Giles, L., Robinson, S.A., Lennon, A.M., Siedow, J.N.: Electron partitioning between the cytochrome and alternative pathways in plant mitochondria, *Plant Physiol.*, 109, 829–837, <https://doi.org/10.1104/pp.109.3.829>, 1995.
- 930 Romero, E., Gómez Castellanos, J.R., Gadda, G., Fraaije, M.W., Mattevi, A.: Same substrate, many reactions: oxygen activation in flavoenzymes, *Chem. Rev.*, 118, 1742–1769, <https://doi.org/10.1021/acs.chemrev.7b00650>, 2018.



- Roth, J., Klinman, J.: Oxygen-18 Isotope Effects as a Probe of Enzymatic Activation of Molecular Oxygen, in: Isotope Effects
935 in Chemistry and Biology, edited by: Kohen, A., Limbach, H.H., CRC Press, Boca Raton, United States, 645–670, 2005.
- Roth, J.P., Klinman, J.P.: Catalysis of electron transfer during activation of O₂ by the flavoprotein glucose oxidase, P. Natl.
Acad. Sci. USA, 100, 62–67, <https://doi.org/10.1073/pnas.252644599>, 2003.
- Severinghaus, J.P., Beaudette, R., Headly, M.A., Taylor, K., Brook, E.J.: Oxygen-18 of O₂ records the impact of abrupt climate
change on the terrestrial biosphere, Science, 324, 1431–1434, <https://doi.org/10.1126/science.1169473>, 2009.
- 940 Sharp, Z.D., Wostbrock, J.A.G., Pack, A.: Mass-dependent triple oxygen isotope variations in terrestrial materials,
Geochemical Perspectives Letters, 7, 27–31, <https://doi.org/10.7185/geochemlet.1815>, 2018.
- Solomon, E.I., Heppner, D.E., Johnston, E.M., Ginsbach, J.W., Cirera, J., Qayyum, M., Kieber-Emmons, M.T., Kjaergaard,
C.H., Hadt, R.G., Tian, L.: Copper active sites in biology, Chem. Rev., 114, 3659–3853,
<https://doi.org/10.1021/cr400327t>, 2014.
- 945 Stolper, D.A., Fischer, W.W., Bender, M.L.: Effects of temperature and carbon source on the isotopic fractionations associated
with O₂ respiration for ¹⁷O/¹⁶O and ¹⁸O/¹⁶O ratios in *E. coli*, Geochim. Cosmochim. Ac., 240, 152–172, <https://doi.org/10.1016/j.gca.2018.07.039>, 2018.
- Strong, P.J., Claus, H.: Laccase: A review of its past and its future in bioremediation, Crit. Rev. Env. Sci. Tec., 41, 373–434,
<https://doi.org/10.1080/10643380902945706>, 2011.
- 950 Su, Q., Klinman, J.P.: Probing the mechanism of proton coupled electron transfer to dioxygen: The oxidative half-reaction of
bovine serum amine oxidase, Biochemistry-US, 37, 12513–12525, <https://doi.org/10.1021/bi981103l>, 1998.
- Sutherland, K.M., Hemingway, J.D., Johnston, D.T.: The influence of reactive oxygen species on “respiration” isotope effects,
Geochim. Cosmochim. Ac., 324, 86–101, <https://doi.org/10.1016/j.gca.2022.02.033>, 2022a.
- Sutherland, K.M., Johnston, D.T., Hemingway, J.D., Wankel, S.D., Ward, C.P.: Revised microbial and photochemical triple-
955 oxygen isotope effects improve marine gross oxygen production estimates, PNAS Nexus, 1,
<https://doi.org/10.1093/pnasnexus/pgac233>, 2022b.
- Tian, G., Berry, J.A., Klinman, J.P.: Oxygen-18 kinetic isotope effects in the dopamine β-monooxygenase reaction: Evidence
for a new chemical mechanism in non-heme, metallomonooxygenase, Biochemistry-US, 33, 226–234,
<https://doi.org/10.1021/bi00167a030>, 1994.
- 960 Tobias, C.R., Böhlke, J.K., Harvey, J.W.: The oxygen-18 isotope approach for measuring aquatic metabolism in high-
productivity waters, Limnol. Oceanogr., 52, 1439–1453, <https://doi.org/10.4319/lo.2007.52.4.1439>, 2007.
- van Berkel, W.J.H., Kamerbeek, N.M., Fraaije, M.W.: Flavoprotein monooxygenases, a diverse class of oxidative biocatalysts,
J. Biotechnol., 124, 670–689, <https://doi.org/10.1016/j.jbiotec.2006.03.044>, 2006.
- Venables, W.N., Ripley, B.D. (Eds.): Modern Applied Statistics with S, Springer New York, United States,
965 <https://doi.org/10.1007/978-0-387-21706-2>, 2002.



- Wang, X., Depew, D., Schiff, S., Smith, R.E.H.: Photosynthesis, respiration, and stable isotopes of oxygen in a large oligotrophic lake (Lake Erie, USA–Canada), *Can. J. Fish. Aquat. Sci.*, 65, 2320–2331, <https://doi.org/10.1139/F08-134>, 2008.
- Wassenaar, L.I., Hendry, M.J.: Dynamics and stable isotope composition of gaseous and dissolved oxygen, *Ground Water*, 45, 447–460, <https://doi.org/10.1111/j.1745-6584.2007.00328.x>, 2007.
- Welford, R.W.D., Lam, A., Mirica, L.M., Klinman, J.P.: Partial conversion of *Hansenula polymorpha* amine oxidase into a “plant” amine oxidase: Implications for copper chemistry and mechanism, *Biochemistry-US*, 46, 10817–10827, <https://doi.org/10.1021/bi700943r>, 2007.
- Werner, R.A., Brand, W.A.: Referencing strategies and techniques in stable isotope ratio analysis, *Rapid Commun. Mass Sp.*, 15, 501–519, <https://doi.org/10.1002/rcm.258>, 2001.
- Wostbrock, J.A.G., Cano, E.J., Sharp, Z.D.: An internally consistent triple oxygen isotope calibration of standards for silicates, carbonates and air relative to VSMOW2 and SLAP2, *Chem. Geol.*, 533, 119432, <https://doi.org/10.1016/j.chemgeo.2019.119432>, 2020.
- Yoshikawa, S., Shimada, A.: Reaction mechanism of cytochrome c oxidase, *Chem. Rev.*, 115, 1936–1989, <https://doi.org/10.1021/cr500266a>, 2015.
- Young, E.D., Galy, A., Nagahara, H.: Kinetic and equilibrium mass-dependent isotope fractionation laws in nature and their geochemical and cosmochemical significance, *Geochim. Cosmochim. Ac.*, 66, 1095–1104, [https://doi.org/10.1016/S0016-7037\(01\)00832-8](https://doi.org/10.1016/S0016-7037(01)00832-8), 2002.
- Zanconato, S., Cooper, D.M., Armon, Y., Epstein, S.: Effect of increased metabolic rate on oxygen isotopic fractionation, *Resp. Physiol.*, 89, 319–327, [https://doi.org/10.1016/0034-5687\(92\)90090-J](https://doi.org/10.1016/0034-5687(92)90090-J), 1992.
- Zhu, H., Peck, S.C., Bonnot, F., et al.: Oxygen-18 kinetic isotope effects of nonheme iron enzymes HEPD and MPnS support iron(III) superoxide as the hydrogen abstraction species, *J. Am. Chem. Soc.*, 137, 10448–10451, <https://doi.org/10.1021/jacs.5b03907>, 2015.